The Gassmann-Burgers model to simulate seismic waves at the Earth crust and mantle

(rheology describing partial melt, seismic anisotropy, attenuation and the brittle-ductile transition (BDT))

José M. Carcione and Flavio Poletto
OGS, Trieste, Italy

Everything in the cosmos is propagated by means of waves

(Manuscript H, 67r, Institut de France, Paris.)

Leonardo da Vinci
(1452-1519)

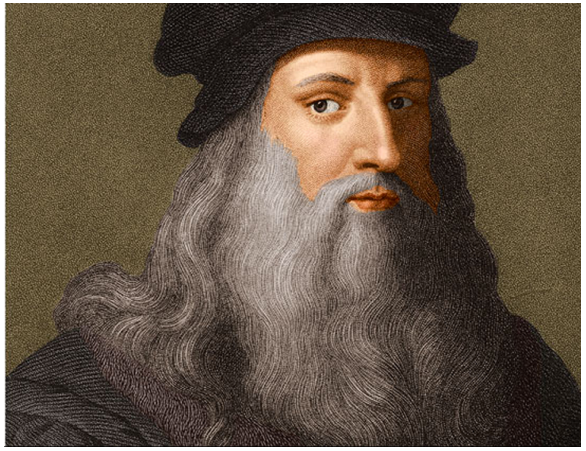

Seismic, electromagnetic, gravitational field

The BDT may be one of the factors that control plate-tectonic activity such as the generation of mountains and plate break-up.

Below this interface, determined by pressure–temperature conditions, aseismic slip activity dominates, since earthquakes cannot be sustained in ductile layers.

The nucleation of earthquakes occurs in the upper brittle part.

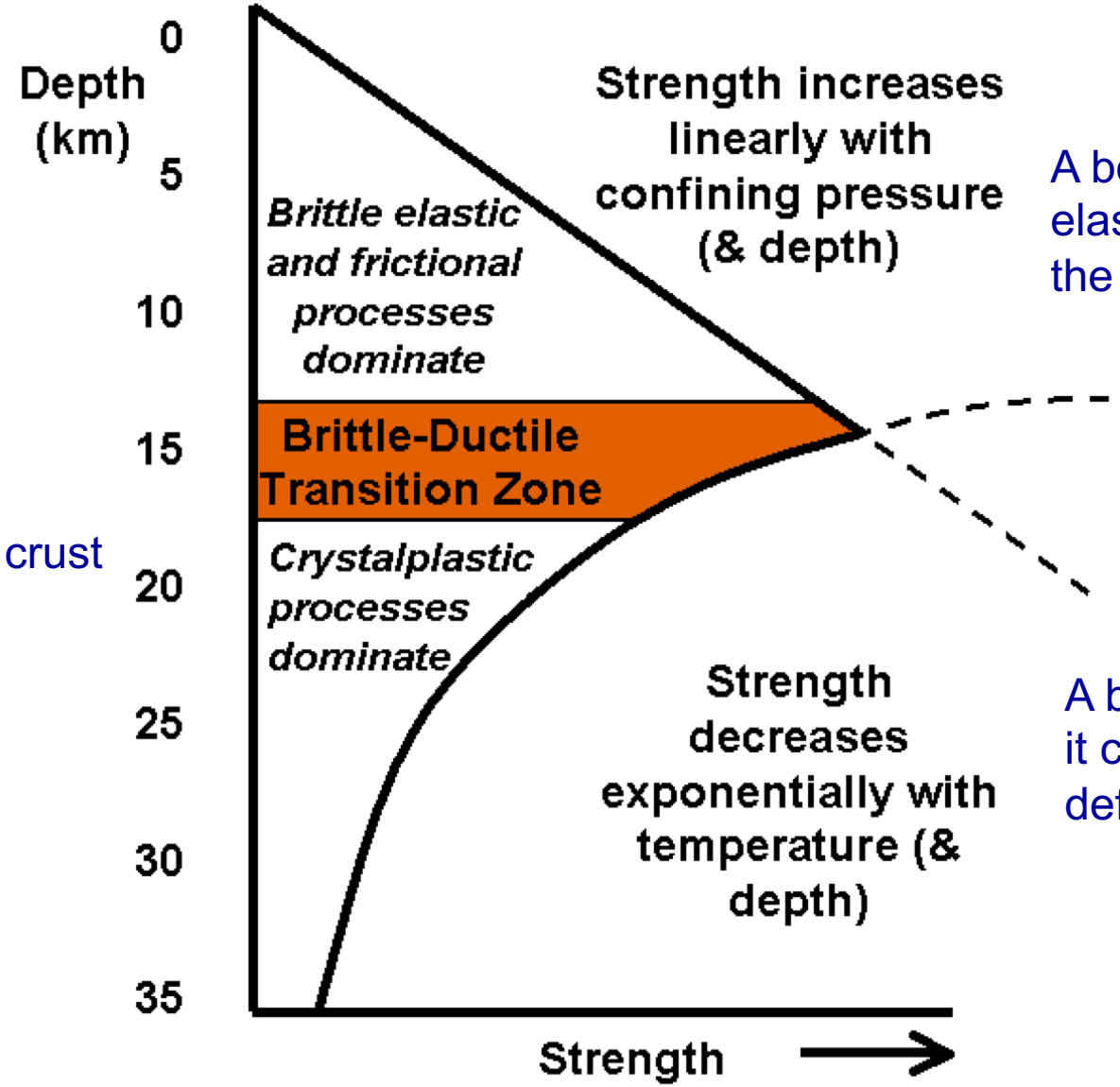

A body behaves as brittle if, after elastic deformation, it reaches soon the critical point of rupture

A body behaves as ductile if instead it can undego a sensible permanent deformation

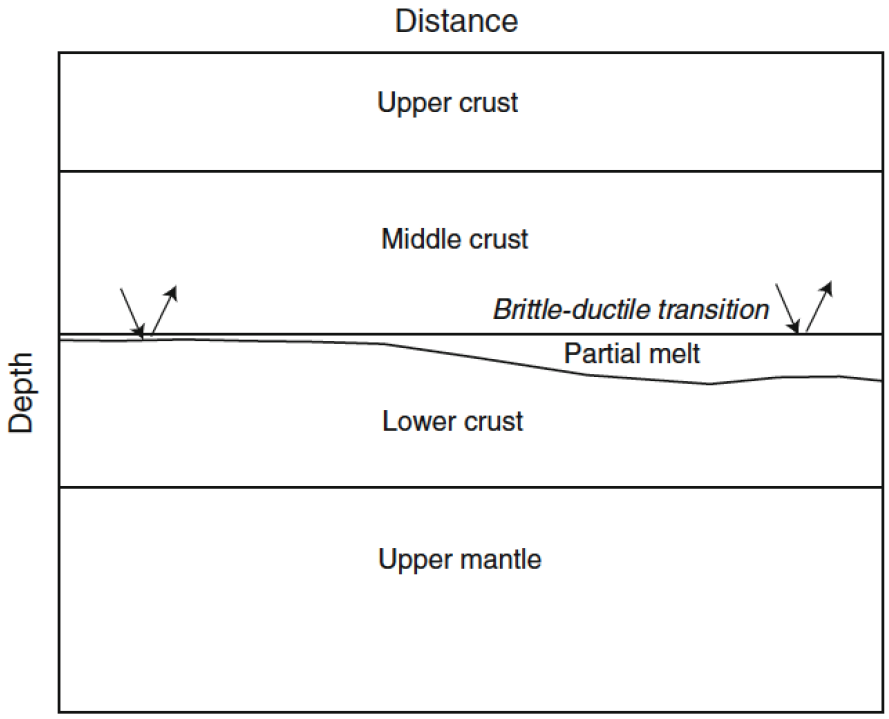

Figure 1
Scheme of the Earth's crust showing possible scenarios of the brittle–ductile transition, namely, reflection from a thin layer (*left*) and a reflection from a single interface (*right*)

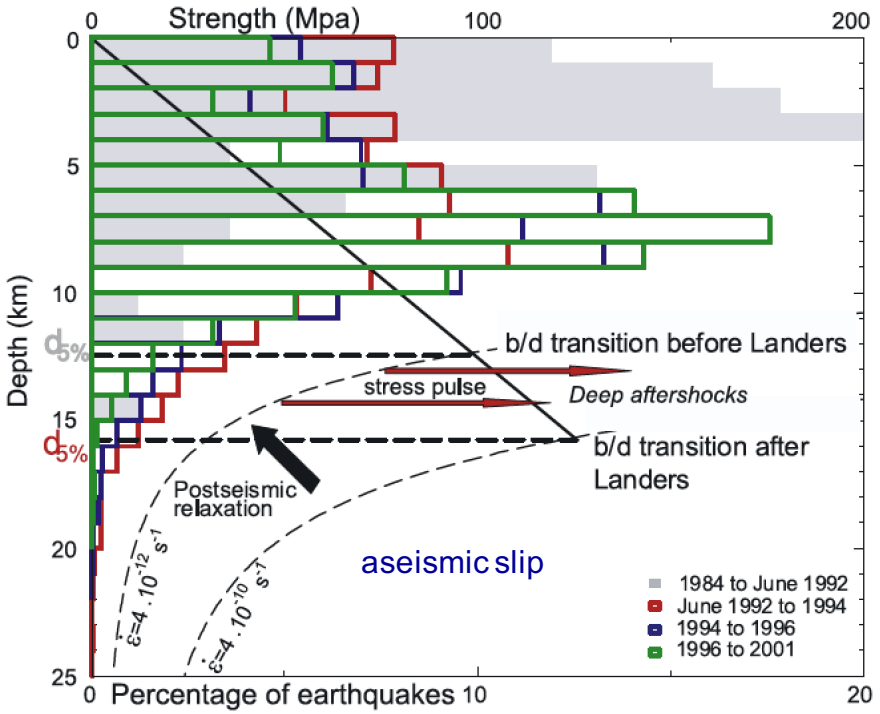

Figure 3. Histograms of the depth distribution of seismicity for different time periods (same intervals as in Figure 1). Overlaid is the strength of the brittle and ductile materials.

Carcione, J. M., and Poletto, F. (2013). *Seismic rheological model and reflection coefficients of the brittle-ductile transition.* Pure and Applied Geophysics, 170, 2021-2035.

After Rolandone et al, 2004

Deep crust seismic line

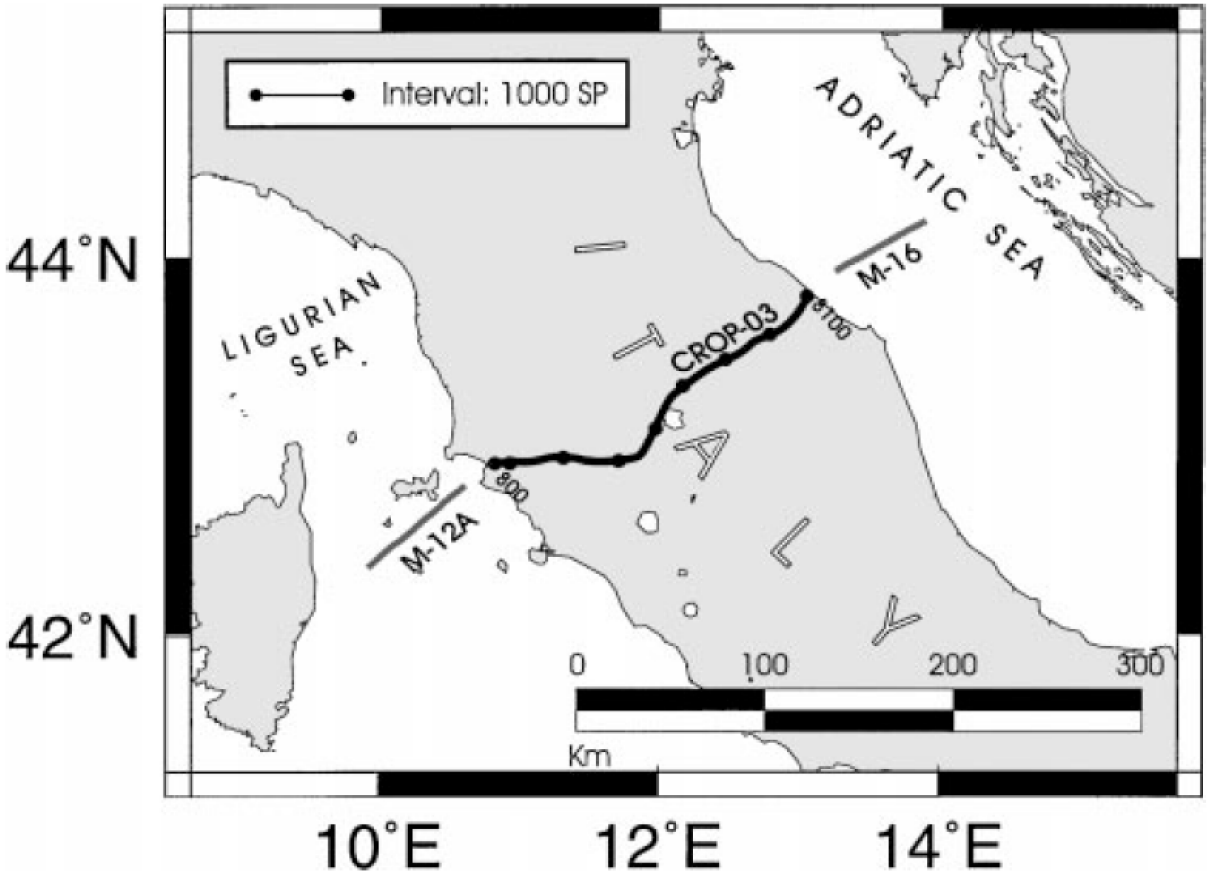

FIG. 1. Location of the CROP-03 seismic line in the northern Apennines.

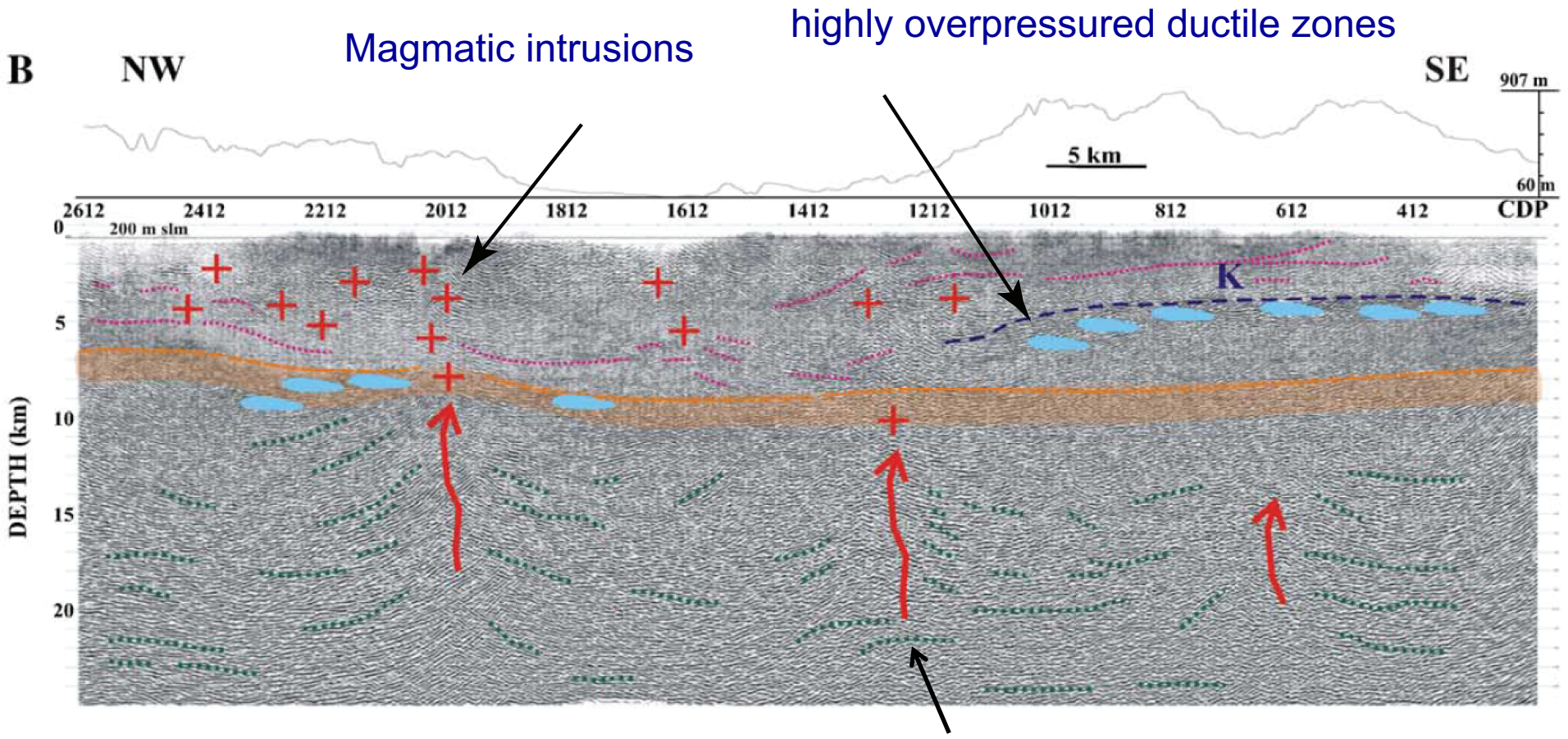

OGS Deep Crust data (Italy)

vertical channels

Accaino et al. (2005). Geofluid evidence from analysis of deep crustal seismic data (Southern Tuscany, Italy). Journal of Volcanology and Geothermal Research 148 (2005) 46–59

Burgers model

it exhibits steady-state creep

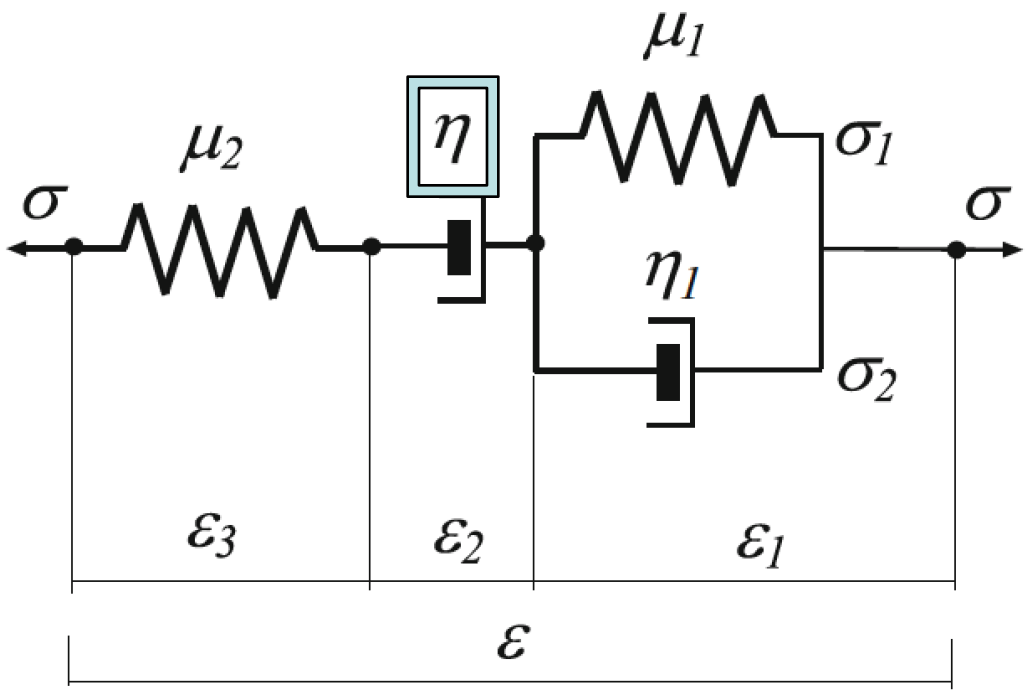

Figure 2
Mechanical representation of the Burgers viscoelastic model for shear deformations (e.g., CARCIONE, 2007). σ, ε, μ, and η represent stress, strain, shear modulus, and viscosity, respectively, where η_1 (Zener viscosity) describes seismic relaxation, while η (Burgers viscosity) is related to plastic flow and processes such as dislocation creep

Carcione, J. M., Helle, H. B., and Gangi, A. F. (2006). *Theory of borehole stability when drilling through salt formations*. Geophysics 71, F31-F47.

We use the octahedral-stress theory to describe the deformation of the ductile layer. In Cartesian coordinates (x, y, z), we define the octahedral stress as

$$\tau_o = \frac{1}{3}\sqrt{(\sigma_v - \sigma_h)^2 + (\sigma_v - \sigma_H)^2 + (\sigma_h - \sigma_H)^2}, \quad (1)$$

where the σ's are the stress components in the principal system, corresponding to the vertical (v) lithostatic stress, and the maximum (H) and minimum (h) horizontal tectonic stresses (see Fig. 3a).

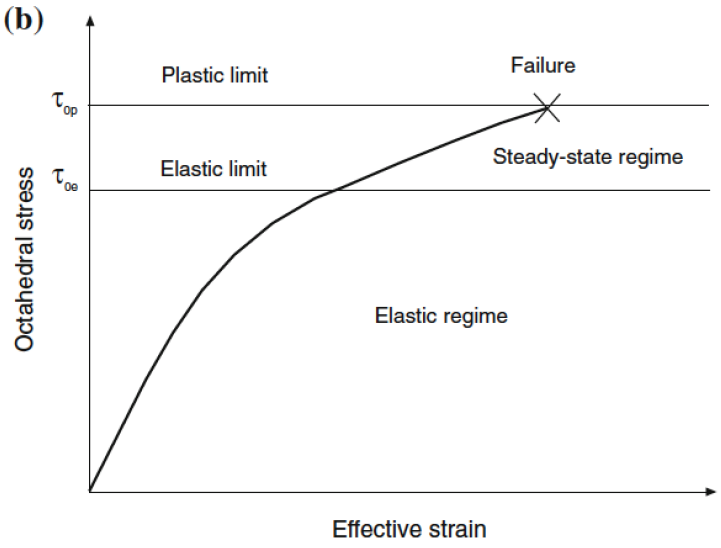

Stress-strain relation

The stress-strain relation is

$$\boldsymbol{\sigma} = \mathbf{P} \cdot \mathbf{e},$$

where

$$\boldsymbol{\sigma} = [\sigma_{11}, \sigma_{22}, \sigma_{33}, \sigma_{23}, \sigma_{13}, \sigma_{12}]^\top$$

is the stress vector,

$$\mathbf{e} = [\epsilon_{11}, \epsilon_{22}, \epsilon_{33}, 2\epsilon_{23}, 2\epsilon_{13}, 2\epsilon_{12}]^\top,$$

is the strain vector and $\mathbf{P}$ is the stiffness matrix

Carcione, J. M., and Cavallini, F. (1994). *A rheological model for anelastic anisotropic media with applications to seismic wave propagation*. Geophys. J. Int. 119, 338-348.

For a transversely isotropic medium with unrelaxed elasticity constants c_{IJ}, the complex stiffness components are

$$
\begin{aligned}
p_{11} &= \Lambda_1(2+a^2)^{-1} + \Lambda_2(2+b^2)^{-1} + \Lambda_4/2 \\
p_{12} &= p_{11} - \Lambda_4 \\
p_{33} &= a^2\Lambda_1(2+a^2)^{-1} + b^2\Lambda_2(2+b^2)^{-1} \\
p_{13} &= a\Lambda_1(2+a^2)^{-1} + b\Lambda_2(2+b^2)^{-1} \\
p_{55} &= \Lambda_3/2 \\
p_{66} &= \Lambda_4/2,
\end{aligned}
$$

where

$$
a = \frac{4c_{13}}{c_{11}+c_{12}-c_{33}+\sqrt{c}}, \qquad b = \frac{4c_{13}}{c_{11}+c_{12}-c_{33}-\sqrt{c}},
$$

and $\Lambda_I(\omega)$, $I = 1,\ldots,4$ are complex and frequency-dependent eigenstiffnesses, given by

$$
\begin{aligned}
\Lambda_1 &= \tfrac{1}{2}(c_{11}+c_{12}+c_{33}+\sqrt{c})M_1 \qquad \text{dilatations} \\
\Lambda_2 &= \tfrac{1}{2}(c_{11}+c_{12}+c_{33}-\sqrt{c})M_2 \\
\Lambda_3 &= 2c_{55}M_2 \qquad \text{shear} \\
\Lambda_4 &= (c_{11}-c_{12})M_2,
\end{aligned}
$$

with

$$
c = 8c_{13}^2 + (c_{11}+c_{12}-c_{33})^2,
$$

$$M_1 = \frac{1 + \mathrm{i}\omega\tau_\epsilon^{(1)}}{1 + \mathrm{i}\omega\tau_\sigma^{(1)}}$$

is a Zener (dilatational) kernel, ω is the angular frequency, with $\mathrm{i} = \sqrt{-1}$, and

$$M_2 = \frac{1 + \mathrm{i}\omega\tau_\epsilon^{(2)}}{1 + \mathrm{i}\omega\tau_\sigma^{(2)} - \frac{\mathrm{i}\mu}{\omega\eta}(1 + \mathrm{i}\omega\tau_\epsilon^{(2)})}$$

is a Burgers (shear) kernel (Carcione, 2007). The quantities τ_σ and τ_ϵ are seismic relaxation times,

$$\mu = \frac{1}{6}(4c_{55} + c_{11} - c_{12}),$$

and η is the flow viscosity describing the ductile behaviour related to shear deformations.

Carcione, J. M., and Poletto, F. (2013). *Seismic rheological model and reflection coefficients of the brittle-ductile transition.* Pure and Applied Geophysics, 170, 2021-2035.

Carcione, J. M., 2014, *Wave Fields in Real Media. Theory and numerical simulation of wave propagation in anisotropic, anelastic, porous and electromagnetic media,* Elsevier. (Third edition, extended and revised).

The viscosity η can be expressed by the Arrhenius equation It is related to the steady-state creep rate $\dot{\epsilon}$ by

$$\eta = \frac{\tau_o}{2\dot{\epsilon}},$$

where τ_o is the octahedral stress. It can be expressed as

$$\dot{\epsilon} = A_\infty \tau_o^n \exp(-E/RT)$$

(Carcione et al., 2006), where A_∞ and n are constants, E is the activation energy, $R = 8.3144$ J/mol/°K is the gas constant and T is the absolute temperature.

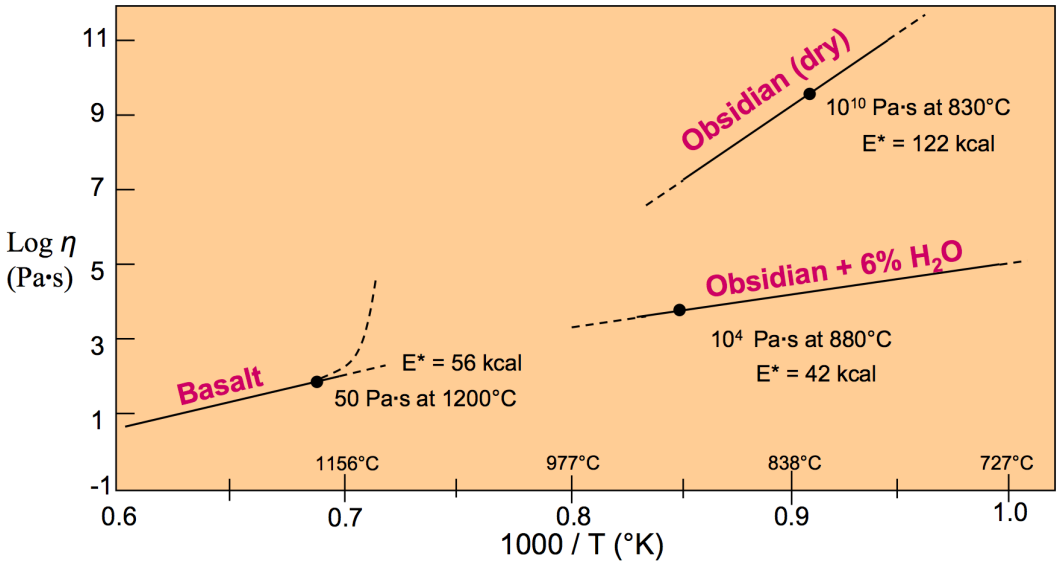

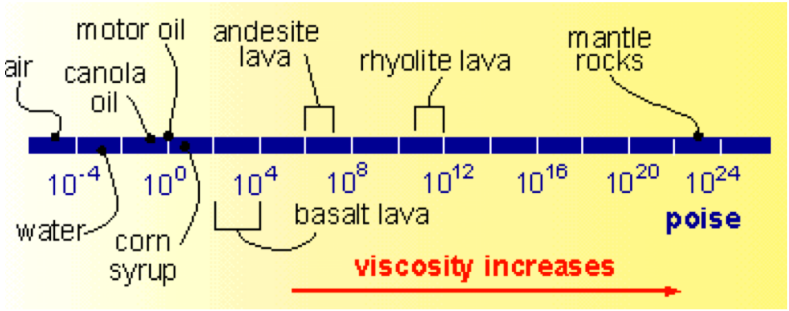

(University of British Columbia)

1 poise = 0.1 Pa s

$$T \to \infty \implies \eta \to 0 \implies \text{ductile} - \text{plastic}\ (M_2 = 0)$$

$$T \to 0 \implies \eta \to \infty \implies \text{brittle}\ (M_2 = 1)$$

elastic

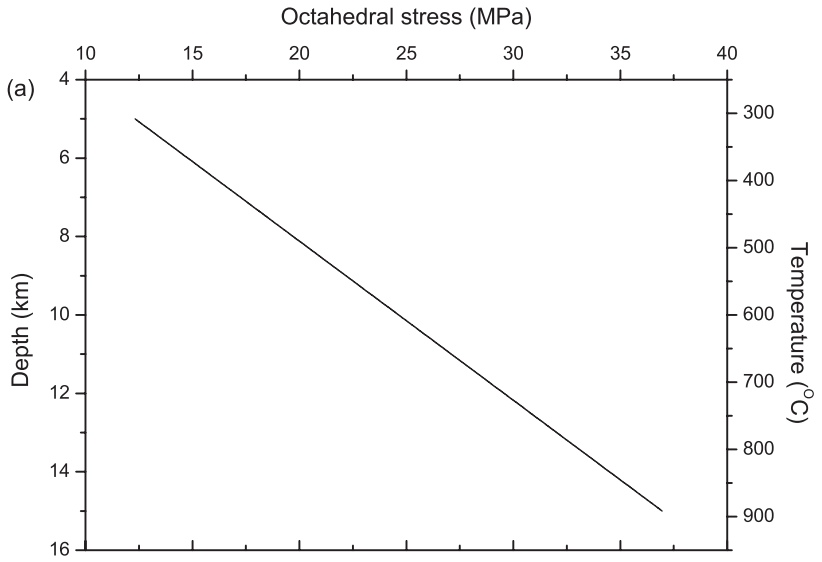

$$\eta = \tau_o^{1-n} A_\infty^{-1} \exp(E/RT)$$

$$A_\infty = 100 \text{ (MPa)}^{-n} \text{ s}^{-1}$$
$$E = 134 \text{ kJ/mol and } n = 2.6$$

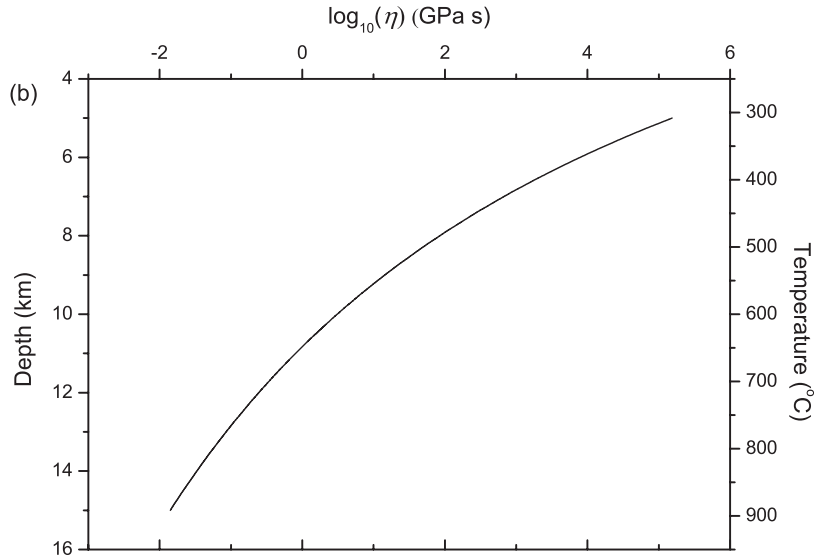

As depth increases, the octahedral stress increases and viscosity decreases

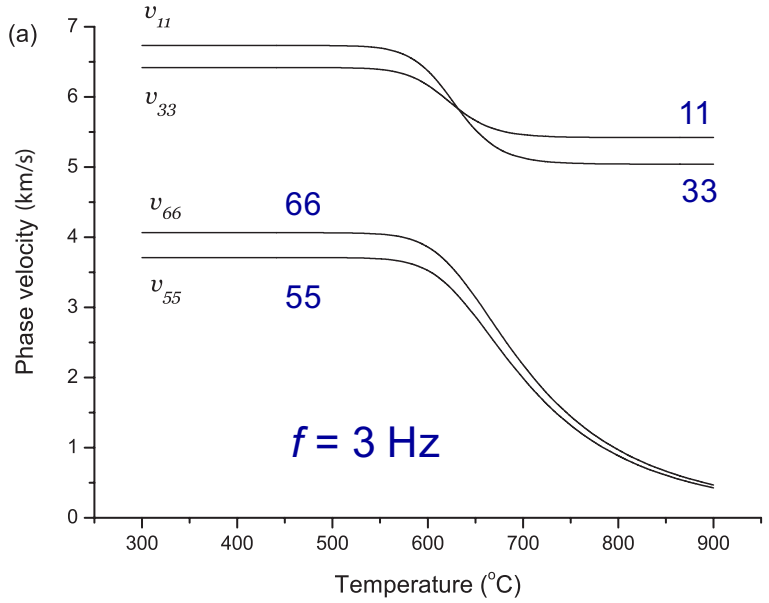

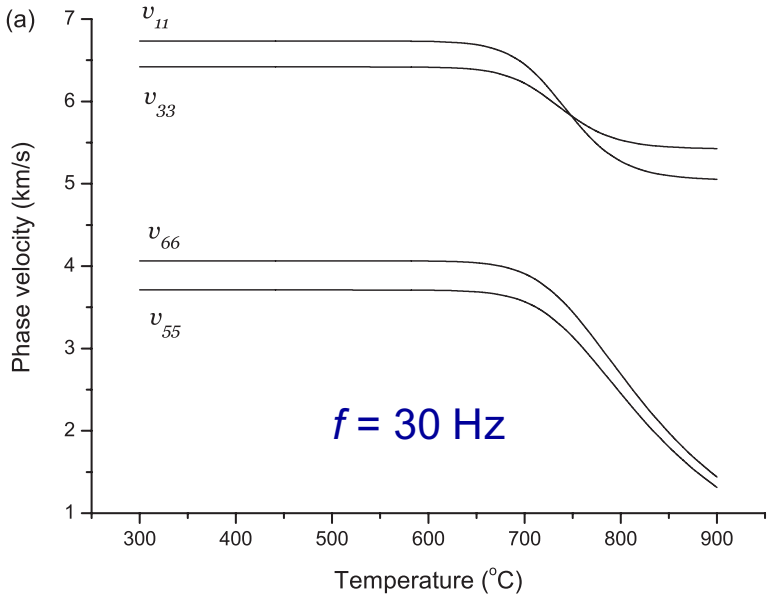

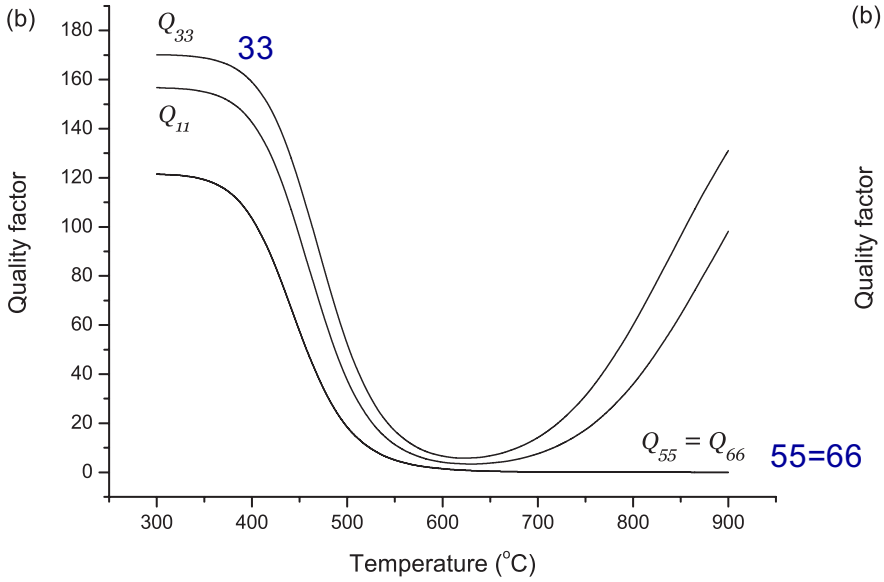

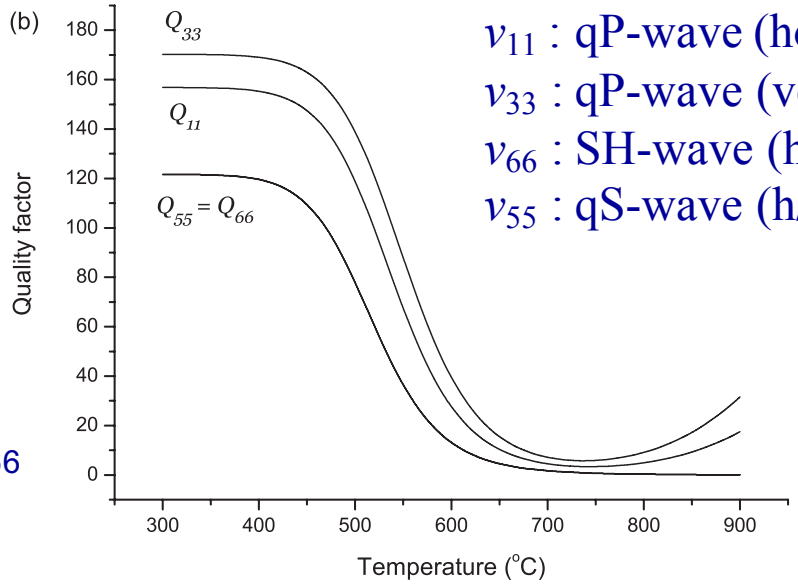

v_{11} : qP-wave (horizontal)
v_{33} : qP-wave (vertical)
v_{66} : SH-wave (horizontal)
v_{55} : qS-wave (h/v)

Critical Burgers viscosity and *T*

$$\bar{\eta} = \sqrt{\frac{q_2}{q_1}} = \frac{\mu}{\omega}\sqrt{\frac{1}{1+N/K}}, \qquad \bar{T}(^\circ\mathrm{C}) = \frac{E}{R\ln\left(2A_\infty \bar{\eta}\tau_0^{n-1}\right)} - 273,$$

$$q_1 = \frac{\omega}{\mu}\left(\frac{K}{N}+1\right),$$

$$q_2 = \frac{\mu}{\omega}\frac{K}{N},$$

$$K = \frac{1}{2}a^2(2+a^2)^{-1}(c_{11}+c_{12}+c_{33}+\sqrt{c}),$$

$$N = \frac{1}{2}b^2(2+b^2)^{-1}(c_{11}+c_{12}+c_{33}-\sqrt{c}).$$

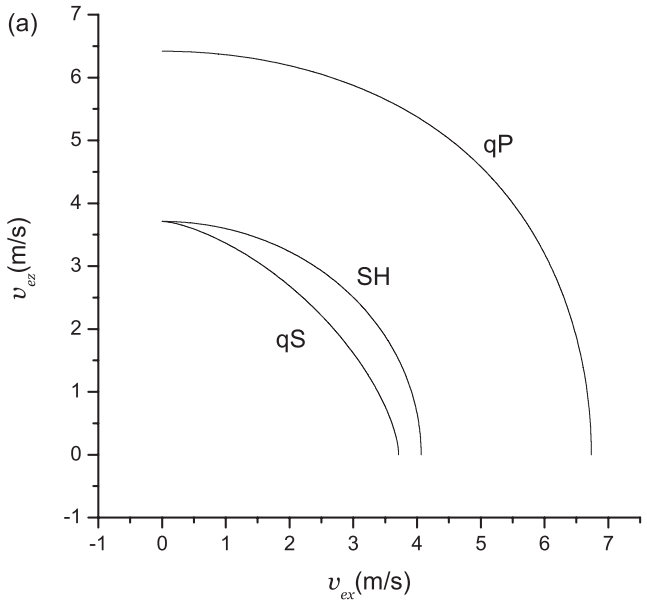

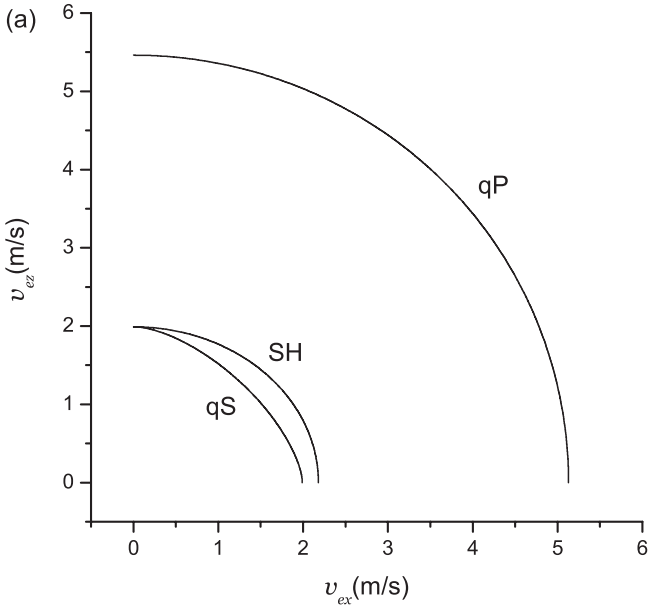

T = 300 ºC, brittle

T = 700 ºC, ductile

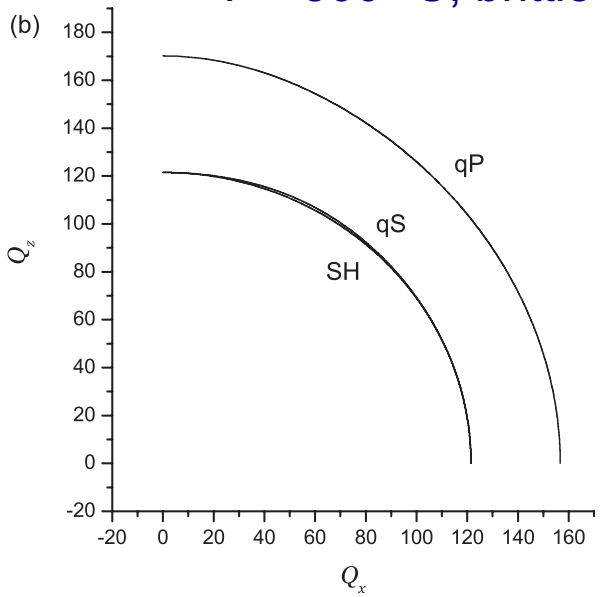

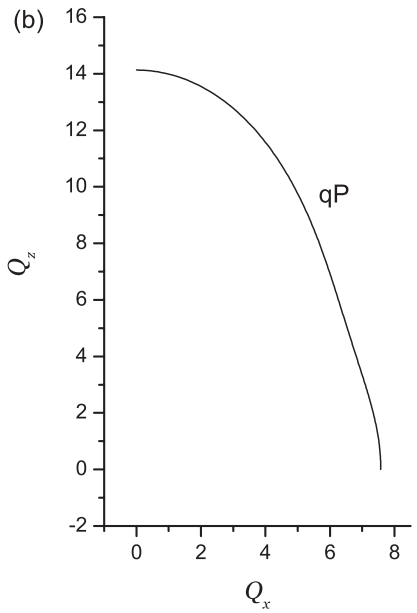

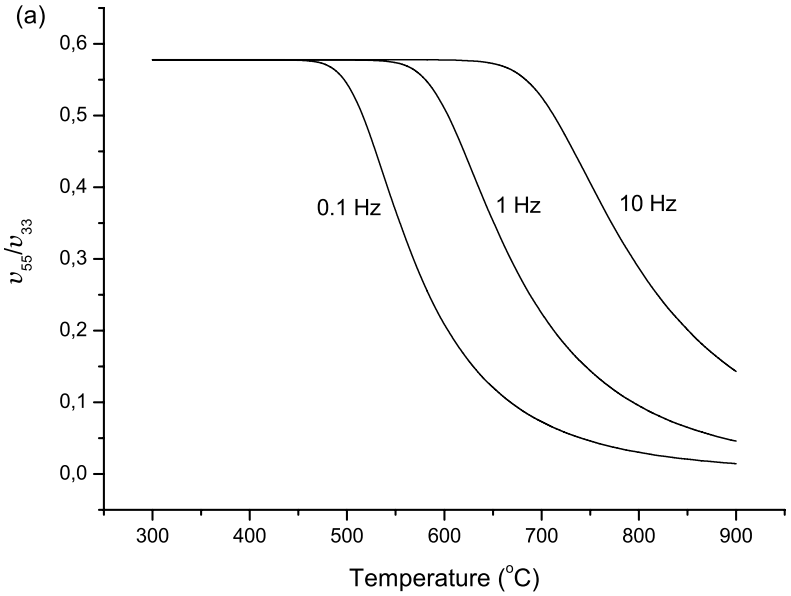

vS/vP wave velocity ratio

At a given *T*, melting occurs at lower frequencies

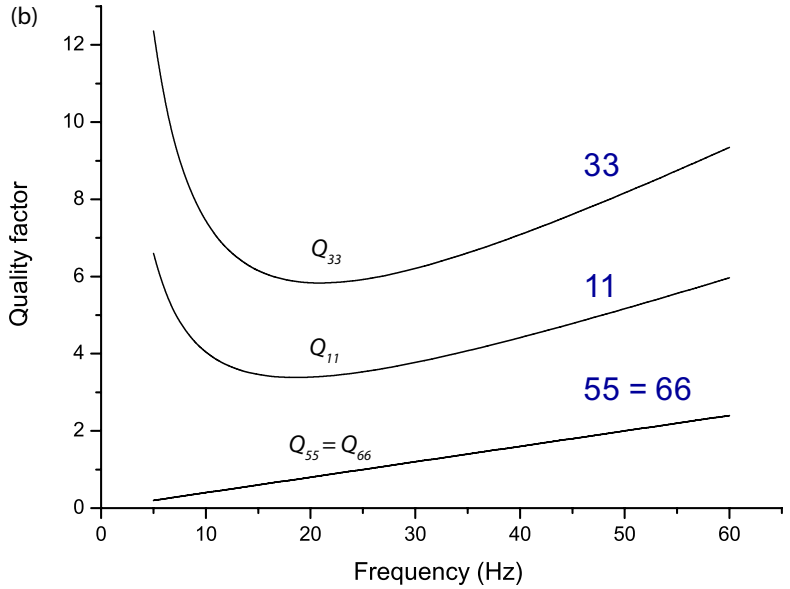

T = 700 ◦C

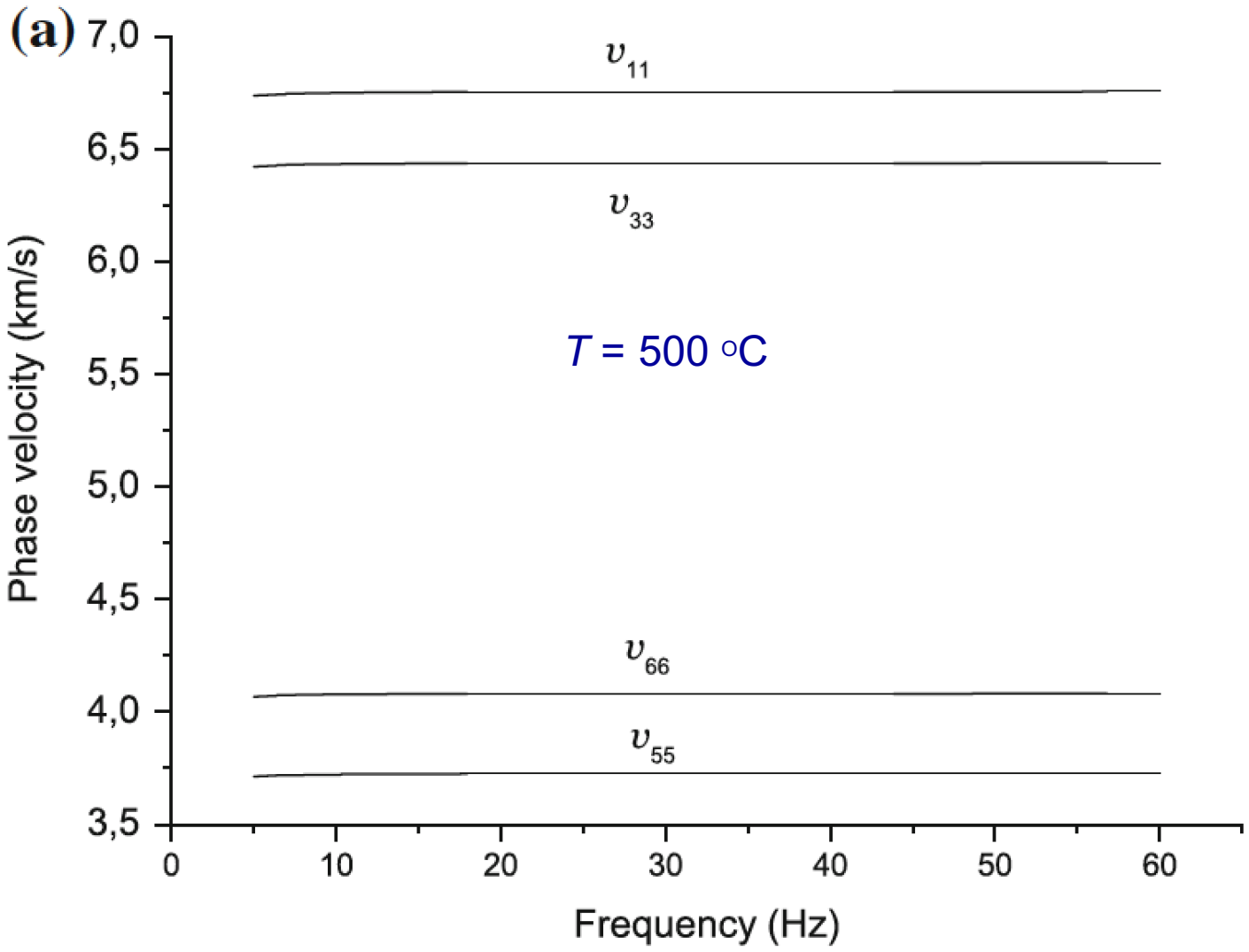
(a)
7,0
6,5
6,0
5,5
5,0
4,5
4,0
3,5
Phase velocity (km/s)
v_{11}
v_{33}
v_{66}
v_{55}
T = 500 ◦C
0
10
20
30
40
50
60
Frequency (Hz)

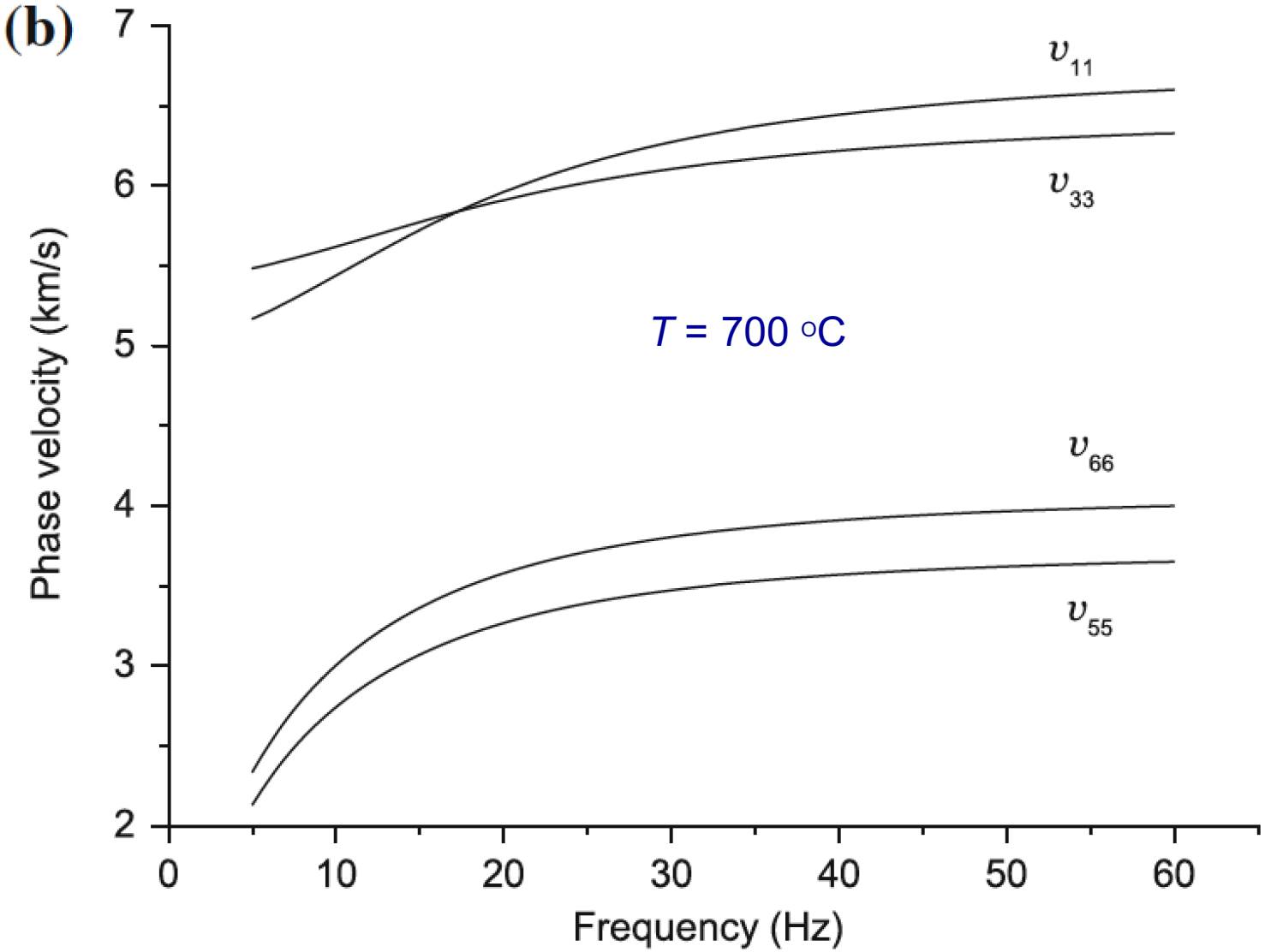
(b)
Phase velocity (km/s)
Frequency (Hz)
v_{11}
v_{33}
v_{66}
v_{55}
T = 700 ◦C
7
6
5
4
3
2
0
10
20
30
40
50
60

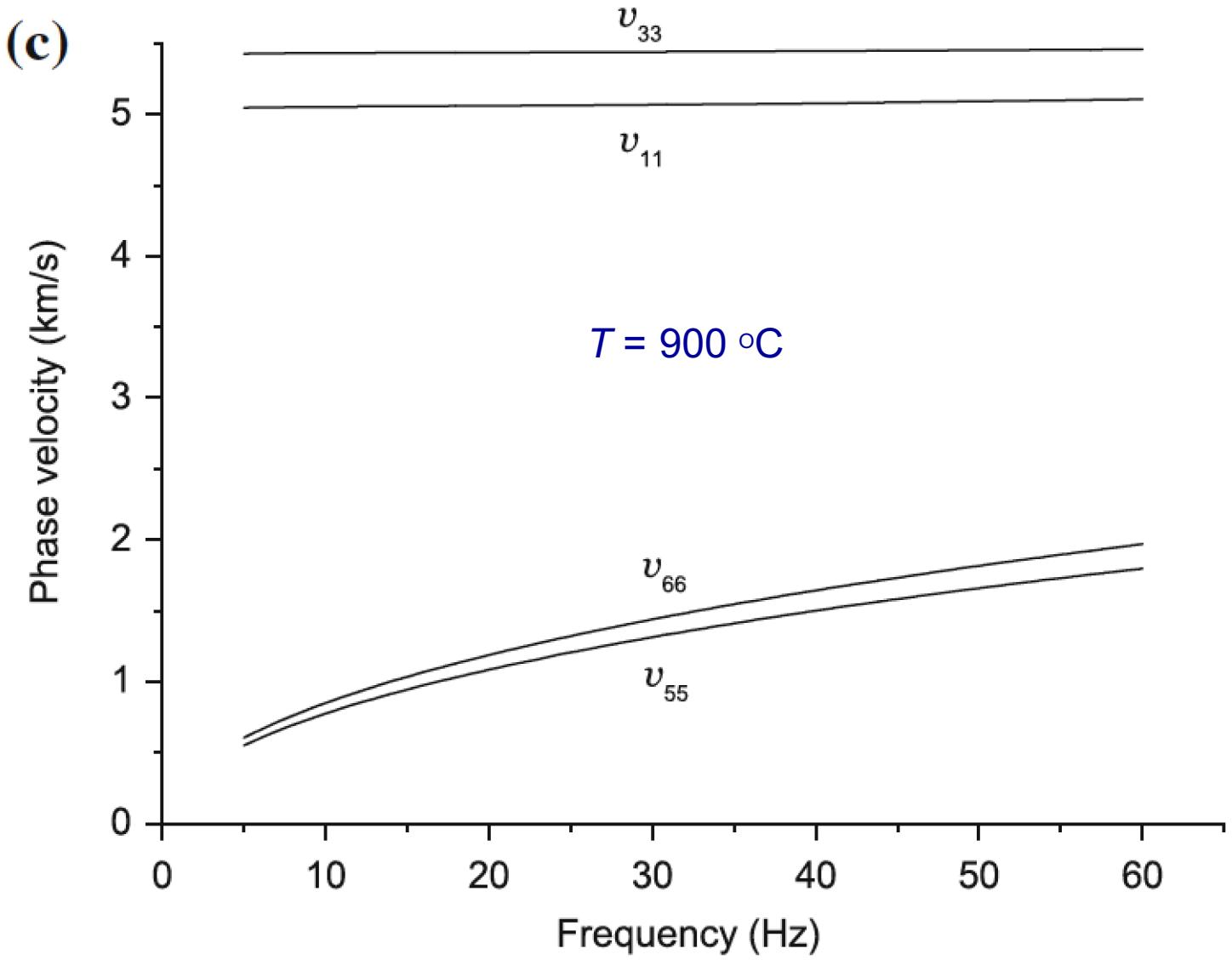
(c)
v_{33}
v_{11}
v_{66}
v_{55}
T = 900 ◦C
Phase velocity (km/s)
Frequency (Hz)
0
1
2
3
4
5
0
10
20
30
40
50
60

The poroelastic case (M_1=1, M_2=μ_B)

$$\mu_B = \frac{\mu_0(1+\mathrm{i}\omega\tau_\epsilon)}{1+\mathrm{i}\omega\tau_\sigma - \frac{\mathrm{i}\mu_0}{\omega\eta}(1+\mathrm{i}\omega\tau_\epsilon)},$$

$$p_e = p_c - np, \qquad \text{Effective pressure = confining - pore}$$

$$K_m = K_0 g_1(p_e), \quad \text{and} \quad \mu_m = \mu_B g_2(p_e), \qquad \text{Dry-rock moduli}$$

$$g_r(p_e) = a_r + b_r p_e - c_r \exp(-p_e/p_r^*), \quad r = 1, 2$$

(Kaselow and Shapiro, 2004; Carcione, 2015)

$$g_r(p_d) = 1 - (1-d_r)\exp(-p_d/p_r^*), \quad r = 1, 2,$$

Gassmann moduli

$$K = K_m + \alpha^2 M \quad \text{and} \quad \mu(\omega) = \mu_m(\omega)$$

wet rock

$$\alpha = 1 - \frac{K_m}{K_s} \quad \text{and} \quad M = \frac{K_s}{1 - \phi - K_m/K_s + \phi K_s/K_f},$$

Φ = porosity
K_σ = Solid modulus
K_ϕ = Fluid modulus

Geothermics and no melt: Jaya, M. S., Shapiro, S. A., Kristinsdóttir, L. H., Bruhn, D., Milsch, H., and Spangenberg, E., 2010, *Temperature dependence of seismic properties in geothermal rocks at reservoir conditions*, Geothermics, 39, 115-123.

Burgers model in the time domain

$$\psi(t) = [A_1 \exp(-t/\tau_1) - A_2 \exp(-t/\tau_2)]H(t),$$

$$\tau_{1,2} = -\frac{1}{\omega_{1,2}} \quad \text{and} \quad A_{1,2} = \frac{\mu_1\mu_2 + \omega_{1,2}\eta_1\mu_2}{\eta_1(\omega_1 - \omega_2)}.$$

$$(2\eta\eta_1)\omega_{1,2} = -b \pm \sqrt{b^2 - 4\mu_1\mu_2\eta\eta_1}, \qquad b = (\mu_1 + \mu_2)\eta + \mu_2\eta_1.$$

$$\mu_1 = \frac{\mu_0\tau_\epsilon}{\tau_\epsilon - \tau_\sigma}, \quad \mu_2 = \mu_0\frac{\tau_\epsilon}{\tau_\sigma}, \quad \eta_1 = \mu_1\tau_\epsilon.$$

$$\dot{v}_x = \frac{1}{\rho}(\partial_x \sigma_{xx} + \partial_z \sigma_{xz}) + s_x,$$

2D PS Euler eqs

$$\dot{v}_z = \frac{1}{\rho}(\partial_x \sigma_{xz} + \partial_z \sigma_{zz}) + s_z$$

8 memory-variable eqs

$$\dot{e}_{ij}^{(l)} = -\frac{1}{\tau_l}(\partial_i v_j + e_{ij}^{(l)}).$$

$$3\dot{\sigma}_{xx} = [3K + 4(A_1 - A_2)]\partial_x v_x + [3K - 2(A_1 - A_2)]\partial_z v_z$$

$$+ 2(2A_1 e_{xx}^{(1)} - 2A_2 e_{xx}^{(2)} - A_1 e_{zz}^{(1)} + A_2 e_{zz}^{(2)}),$$

Stress-strain eqs

$$3\dot{\sigma}_{zz} = [3K + 4(A_1 - A_2)]\partial_z v_z + [3K - 2(A_1 - A_2)]\partial_x v_x$$

$$+ 2(2A_1 e_{zz}^{(1)} - 2A_2 e_{zz}^{(2)} - A_1 e_{xx}^{(1)} + A_2 e_{xx}^{(2)}),$$

$$\dot{\sigma}_{xz} = (A_1 - A_2)(\partial_x v_z + \partial_z v_x) + A_1(e_{xz}^{(1)} + e_{zx}^{(1)}) - A_2(e_{xz}^{(2)} + e_{zx}^{(2)}).$$

Numerical method

Direct grid algorithm (space-time domain)

Time stepping: 4th-order Runge Kutta scheme

Spatial derivatives: Fourier pseudospectral method

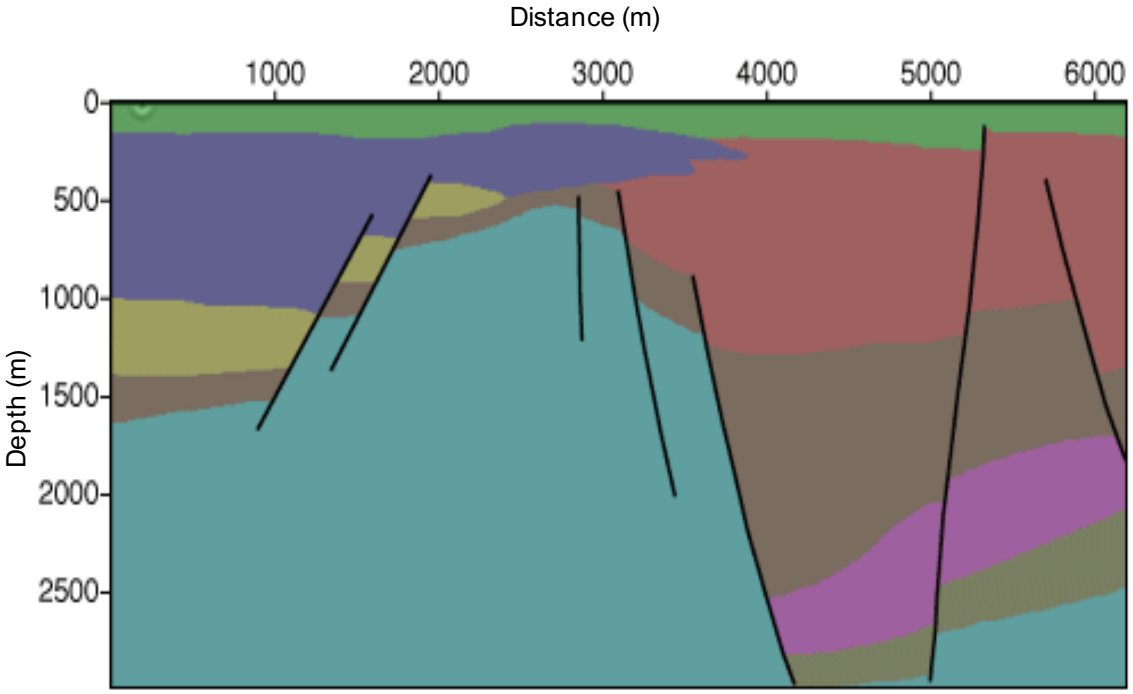

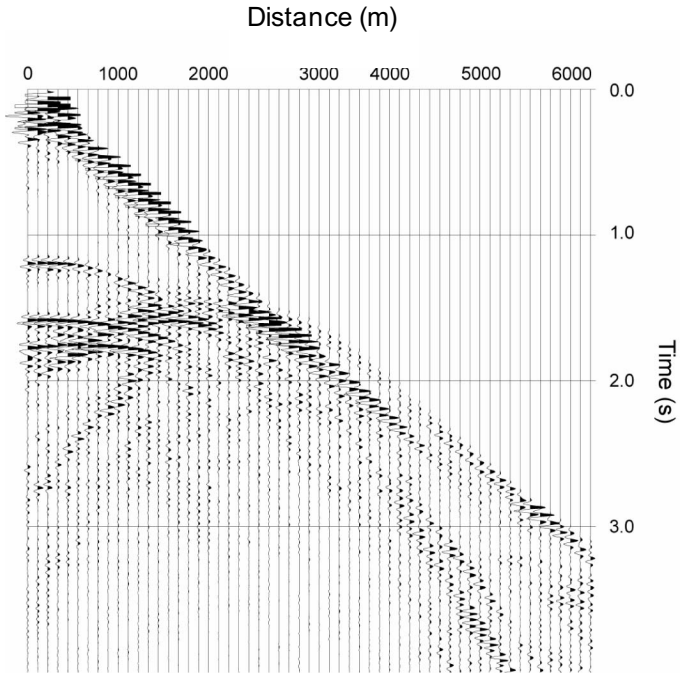

Check with analytical solution

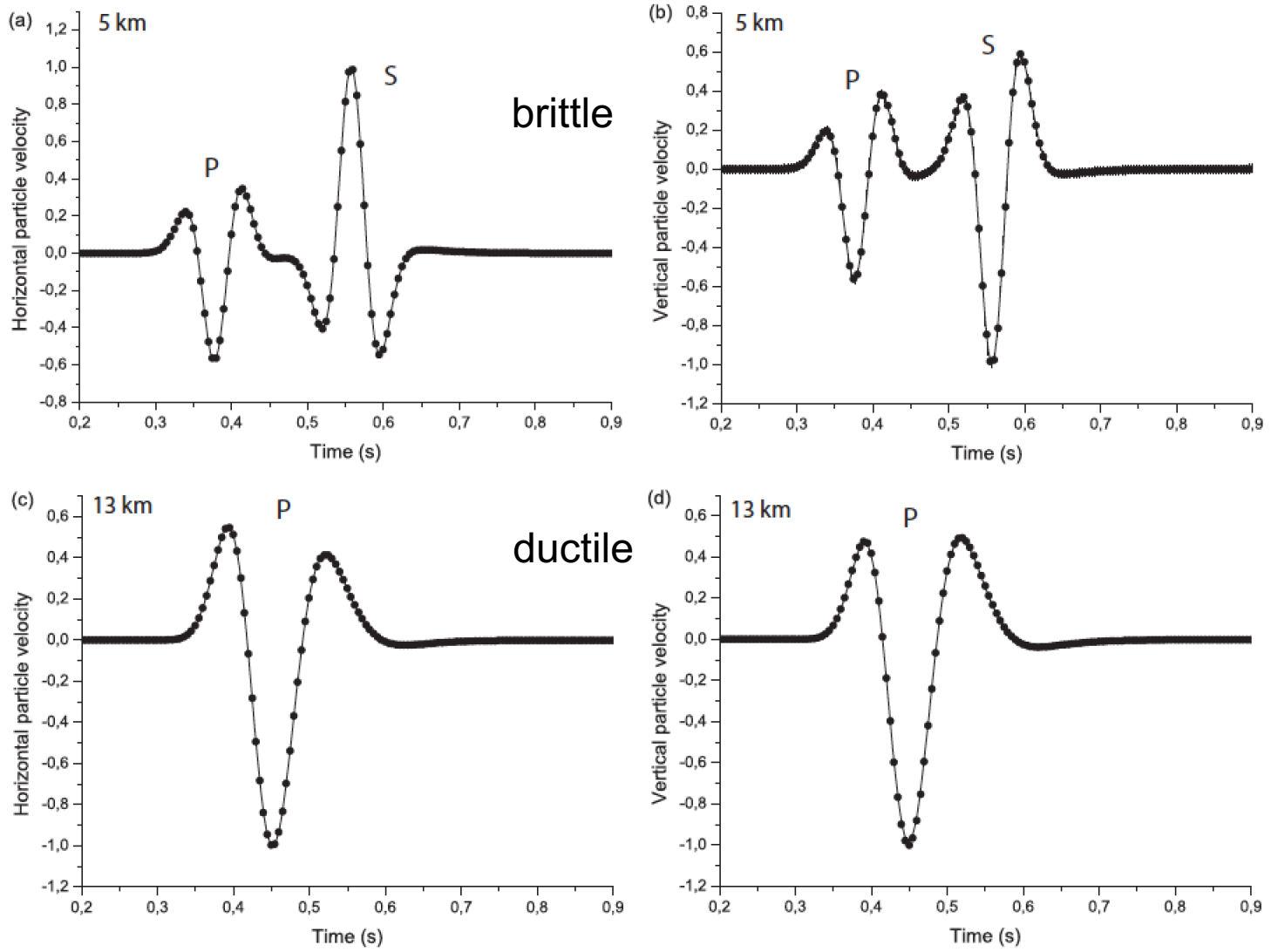

Temperature gradient

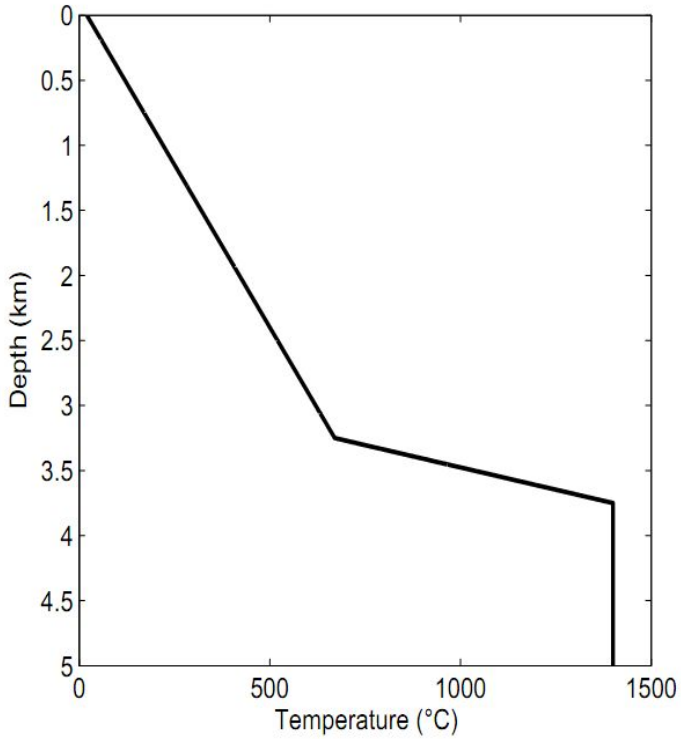

Temperature profile used in the calculation, with a steep gradient at depth, similar to that reported in Foulger (1995)

Iceland rheological model

The Burgers viscosity

Glass-free basaltic rock

$$\dot{\varepsilon} = A_{\infty}\tau_o^n \exp(-E/RT),$$

$$A_{\infty} = 10^{30}\,\mathrm{MPa}^{-n}s^{-1}$$

$$n = 3.5$$

$$E = 990\,\mathrm{kJmol}^{-1}$$

(Violay et al., 2012)

Homogeneous medium:

$V_p = 6$ km/s

$V_s = 3.464$ km/s

$\rho = 2600$ kg/m^3

$Q_0 = 120$

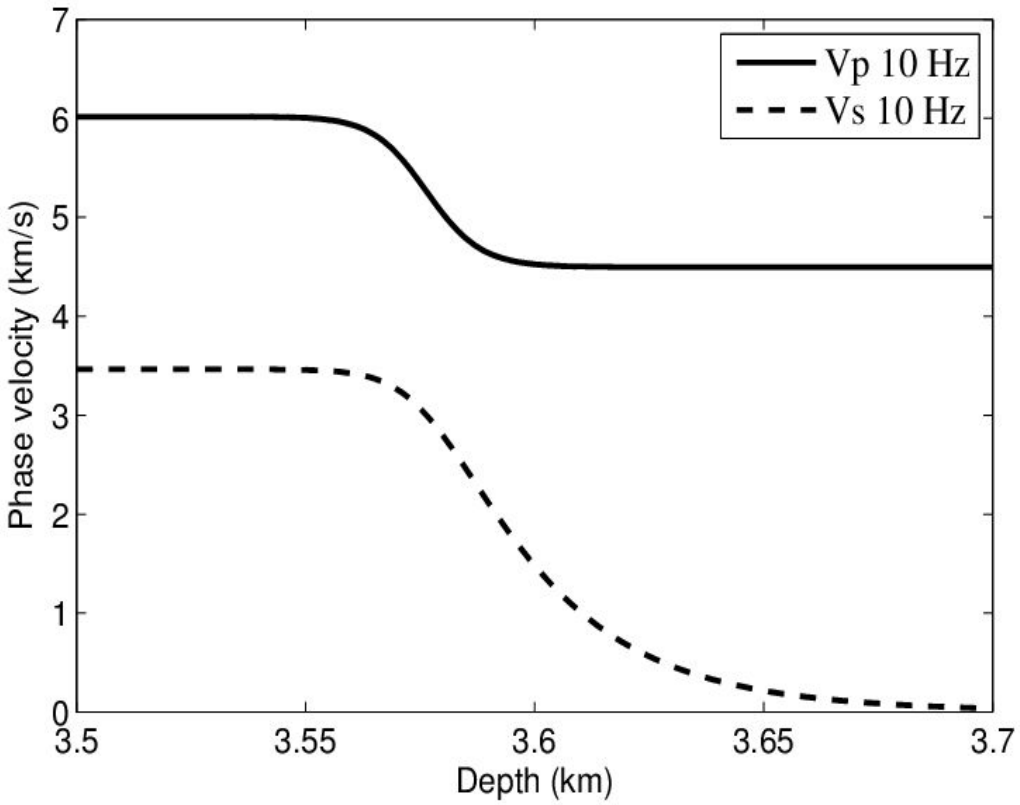

Phase-velocity profiles as a function of temperature at 10 Hz

Surface shot simulation

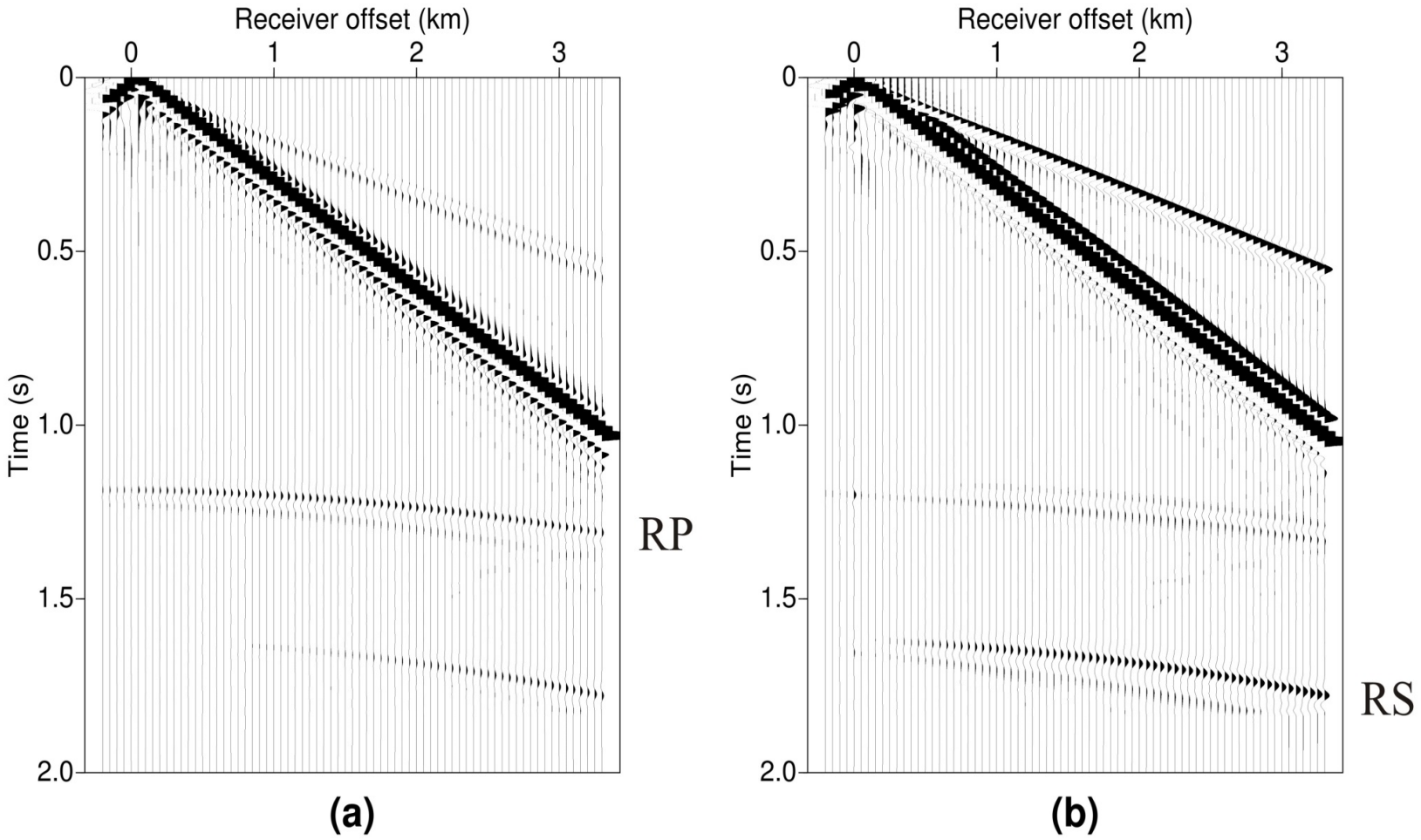

Temperature plume

- Homogeneous, Poisson medium with an unrelaxed P-wave velocity of 6 km/s, density of 2700 kg/m^3, seismic quality factor Q_0 = 120.
- The source is a vertical force with a peak frequency f_p=50 Hz
- Arrhenius constants A_∞=10^{30} MPa^{-n}s^{-1} n=3.5
- Activation energy E=900 kJ/mol

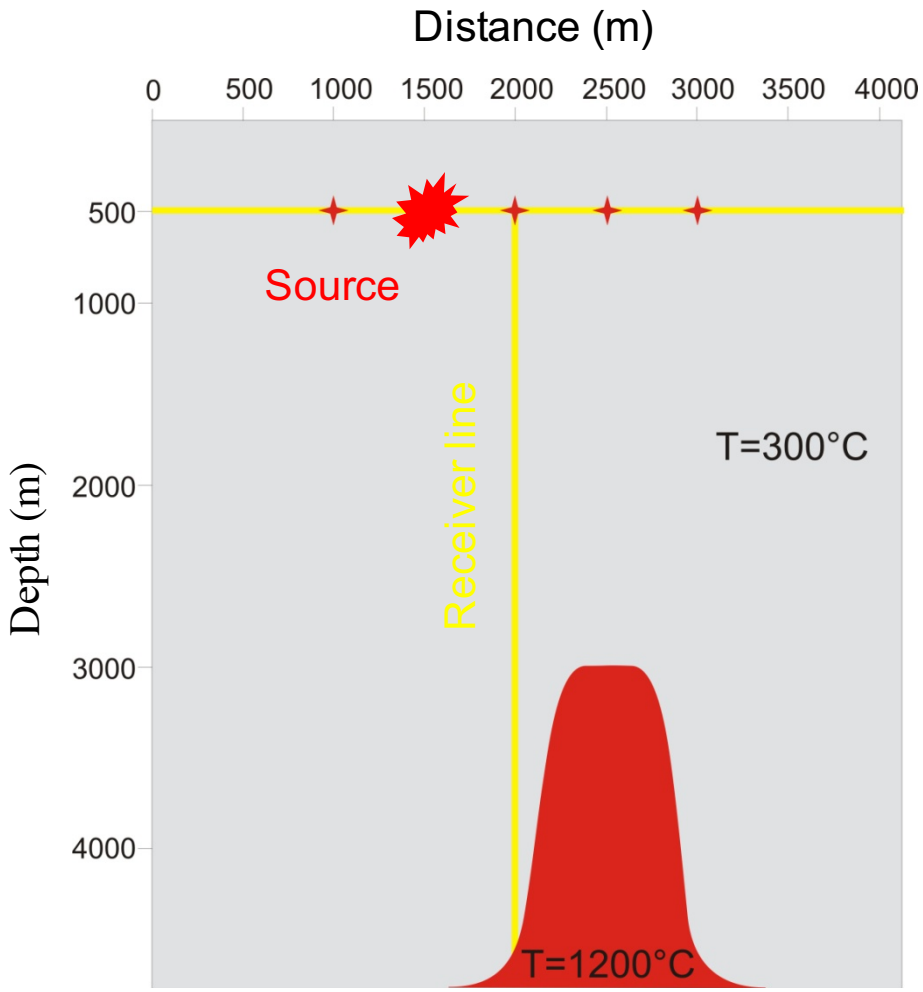

- Model dimension: 4080 x 4760 m. The numerical mesh has 408 x 476 grid points and a unifrom grid spacing of 10 m
- The time step is 2.0E-4 s
- The maximum time propagation 1.5 s
- Source duration: 120 ms

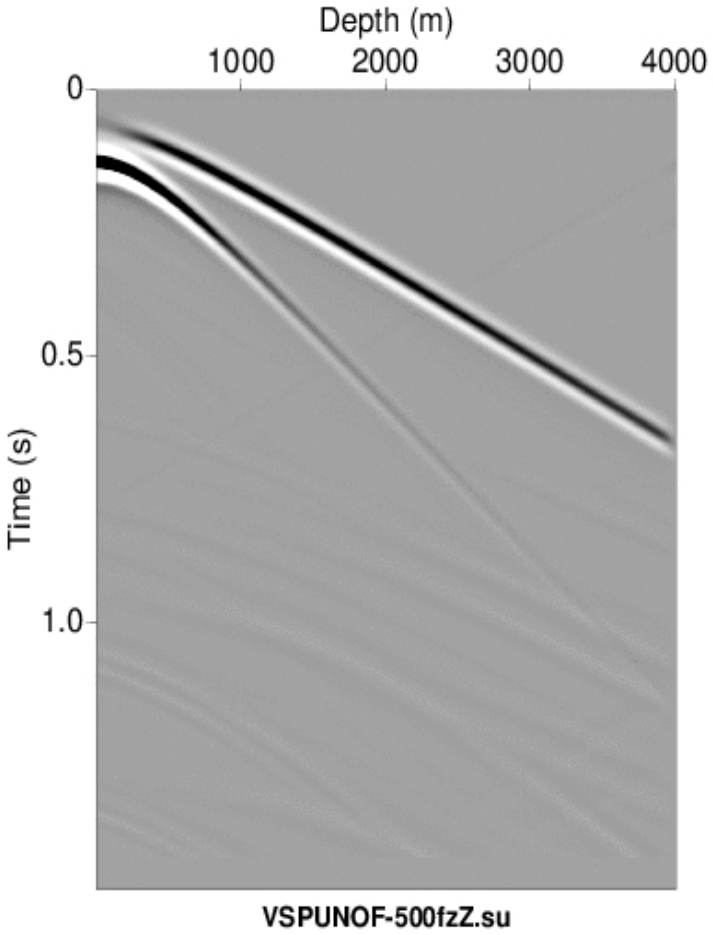
Depth (m)
1000
2000
3000
4000
0
0.5
1.0
Time (s)
VSPUNOF-500fzZ.su

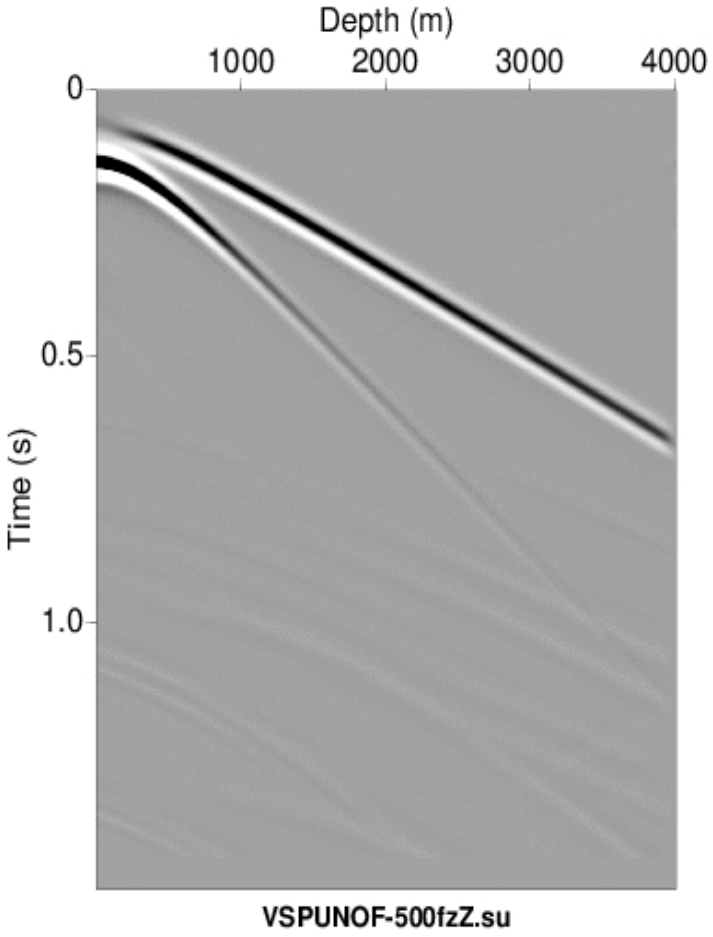
Depth (m)
1000
2000
3000
4000
0
0.5
1.0
Time (s)
VSPUNOF-500fzZ.su

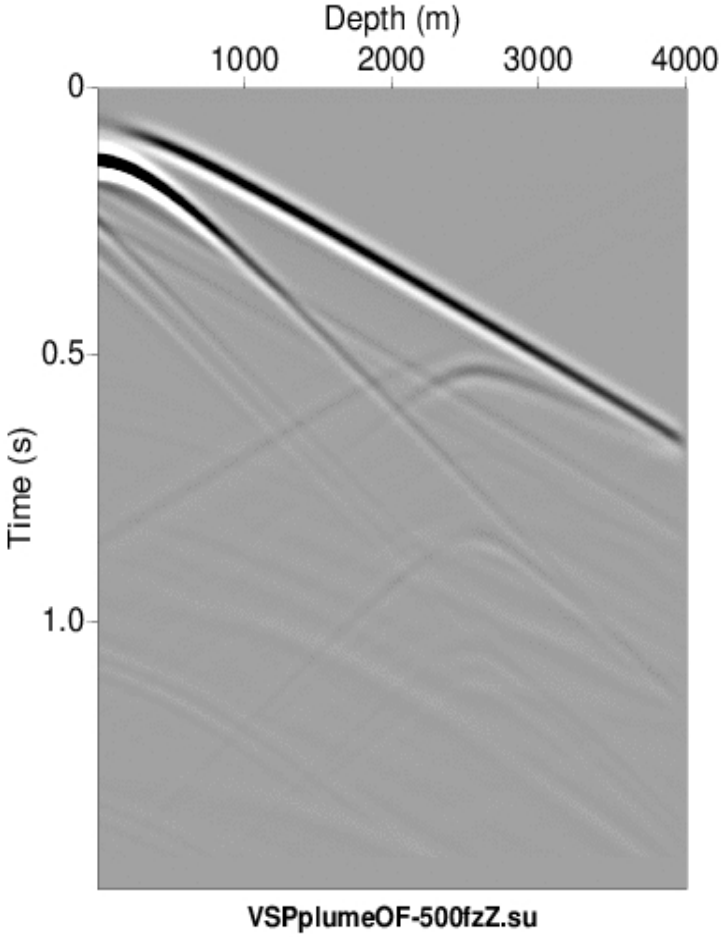
Depth (m)
1000
2000
3000
4000
0
0.5
1.0
Time (s)
VSPplumeOF-500fzZ.su

VSP

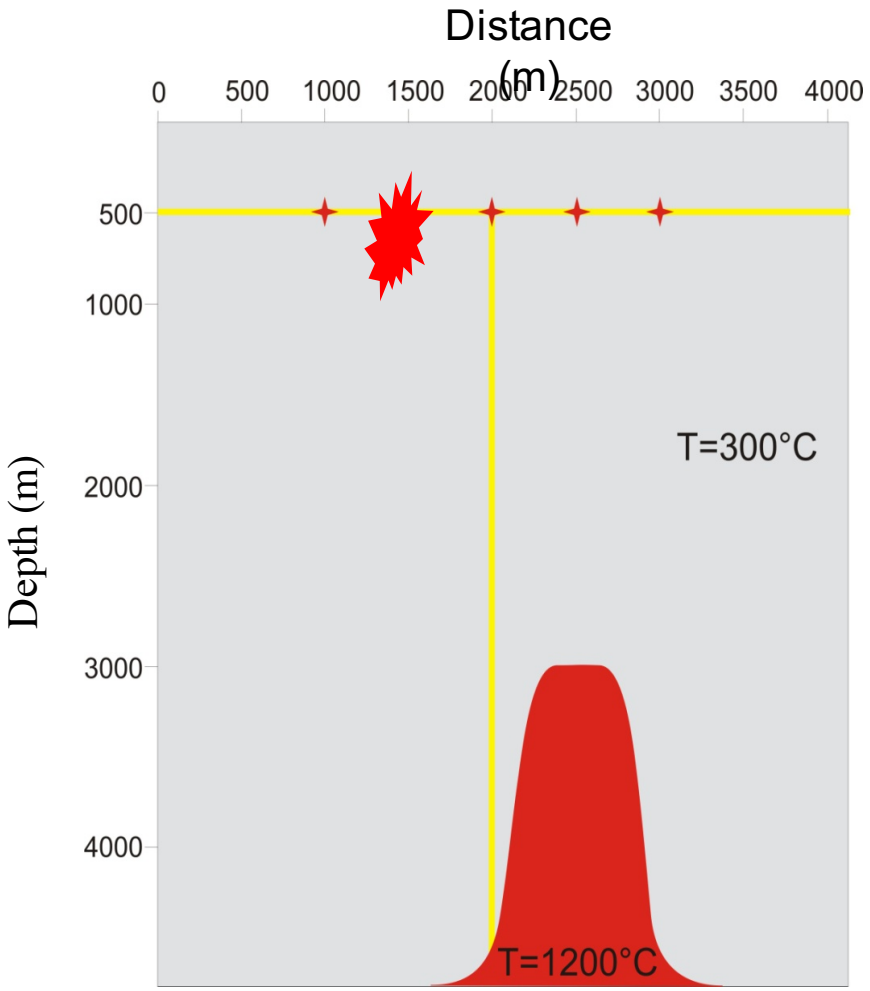
Distance
(m)
0
500
1000
1500
2000
2500
3000
3500
4000
Depth (m)
500
1000
2000
3000
4000
T=300°C
T=1200°C

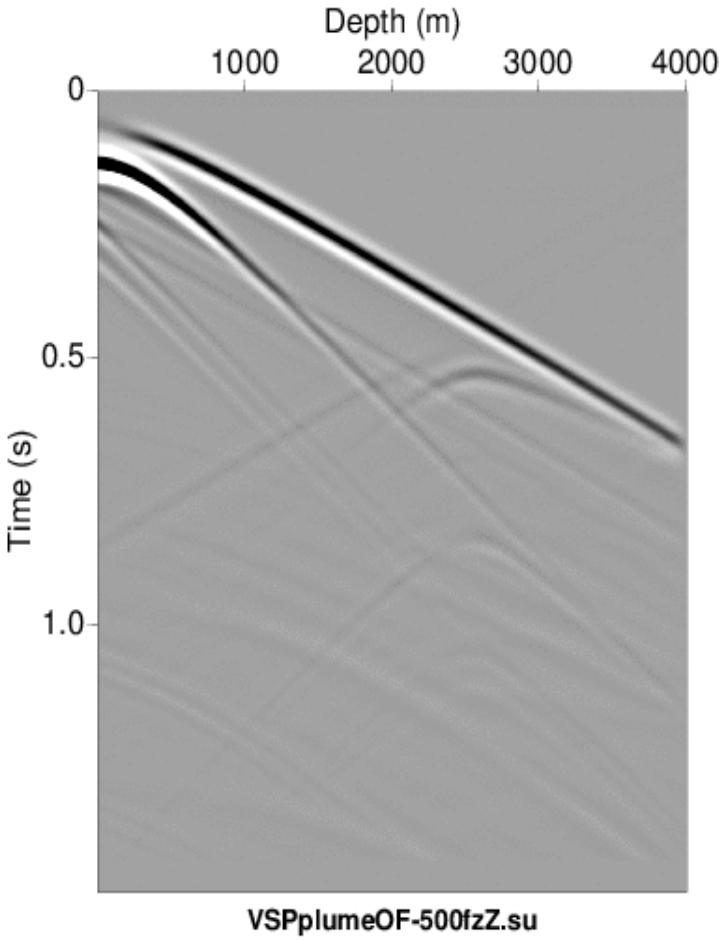
Depth (m)
1000
2000
3000
4000
0
0.5
1.0
Time (s)
VSPplumeOF-500fzZ.su

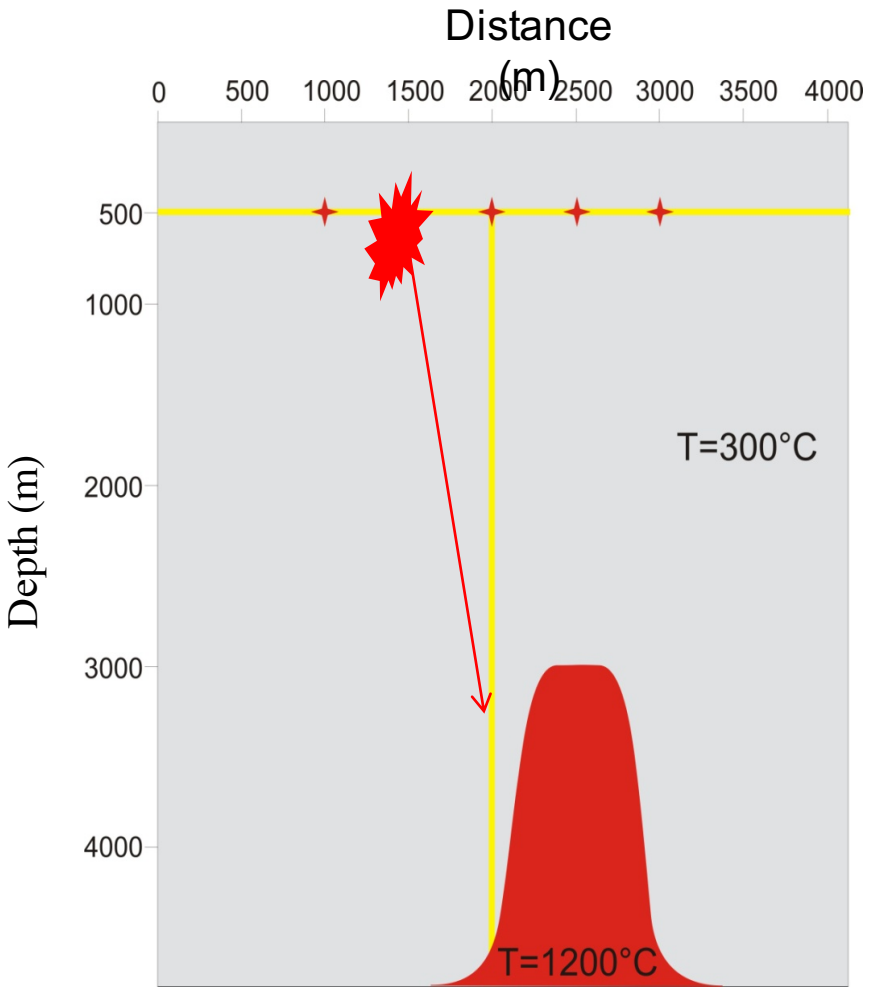
Distance
(m)
0
500
1000
1500
2000
2500
3000
3500
4000
Depth (m)
500
1000
2000
3000
4000
T=300°C
T=1200°C

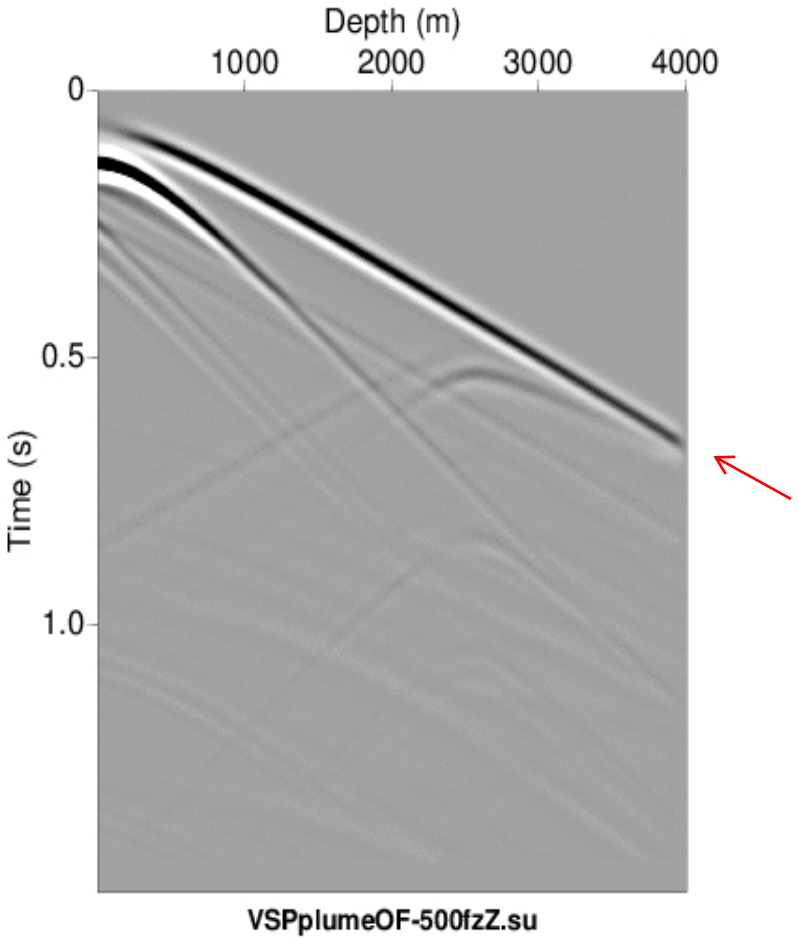
Depth (m)
1000
2000
3000
4000
0
0.5
1.0
Time (s)
VSPplumeOF-500fzZ.su

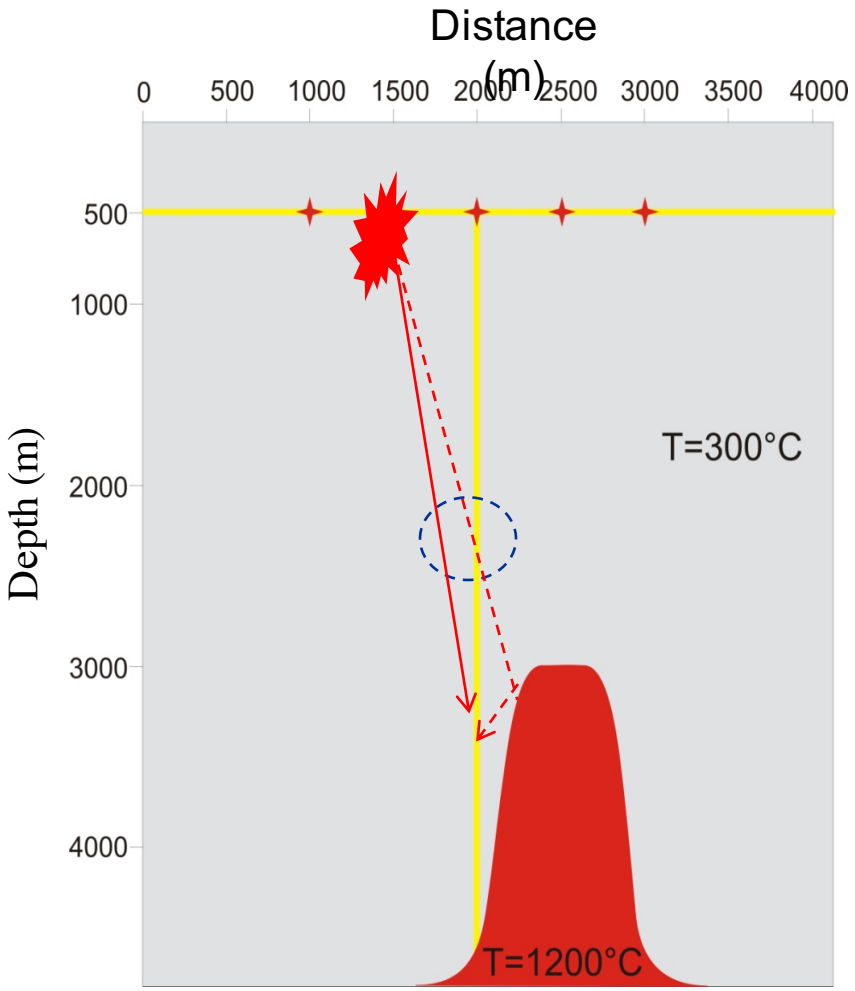
Distance
(m)
0
500
1000
1500
2000
2500
3000
3500
4000
Depth (m)
500
1000
2000
3000
4000
T=300°C
T=1200°C

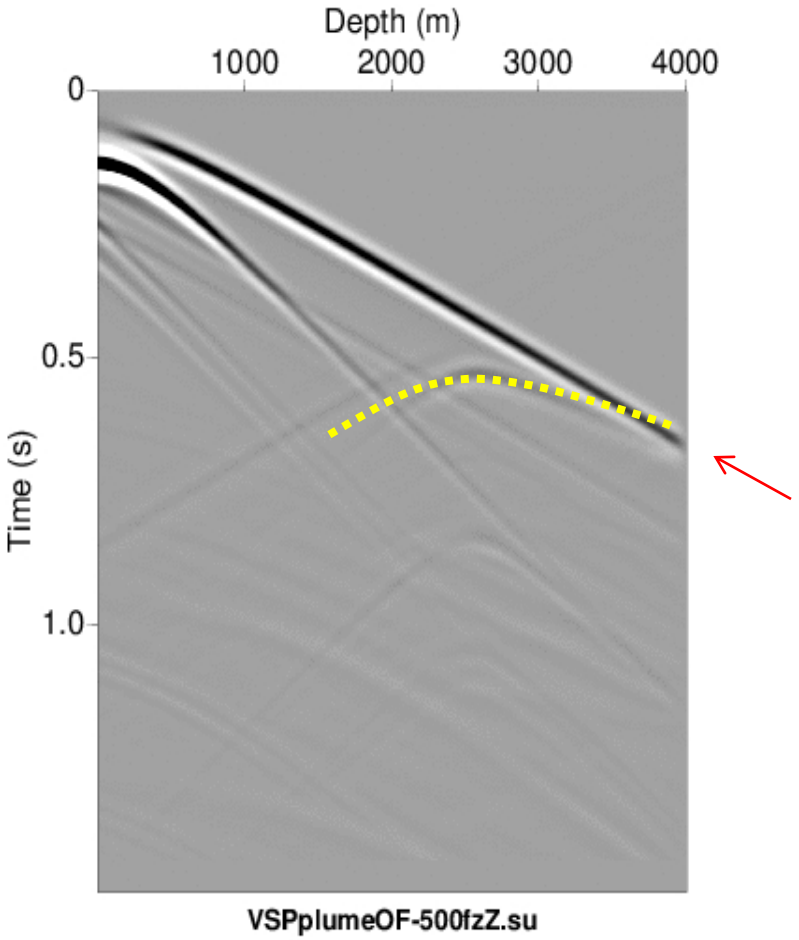
Depth (m)
1000
2000
3000
4000
0
0.5
1.0
Time (s)
VSPplumeOF-500fzZ.su

Amphibolite (Popp and Kern, 1994)

Table 1. Wave velocities versus confining pressure.

Pressure (MPa)	v_P (dry) (km/s)	v_S (dry) (km/s)	v_P (wet) (km/s)	v_S (wet) (km/s)
0.1	4.50	2.82	5.90	3
12	4.91	3.13	6.21	3.35
20	5.30	3.25	6.30	3.45
35	5.60	3.35	6.45	3.55
50	5.84	3.45	6.51	3.60
100	6.25	3.65	6.62	3.70
125	6.40	3.75	6.68	3.75
150	6.50	3.80	6.70	3.78
200	6.62	3.86	6.78	3.82
250	6.66	3.90	6.80	3.85
300	6.70	3.91	6.82	3.86
350	6.75	3.92	–	–
400	6.80	3.93	–	–
450	6.82	3.93	–	–
500	6.85	3.94	–	–
550	6.88	3.95	–	–
600	6.90	3.95	–	–

Theory and experiment

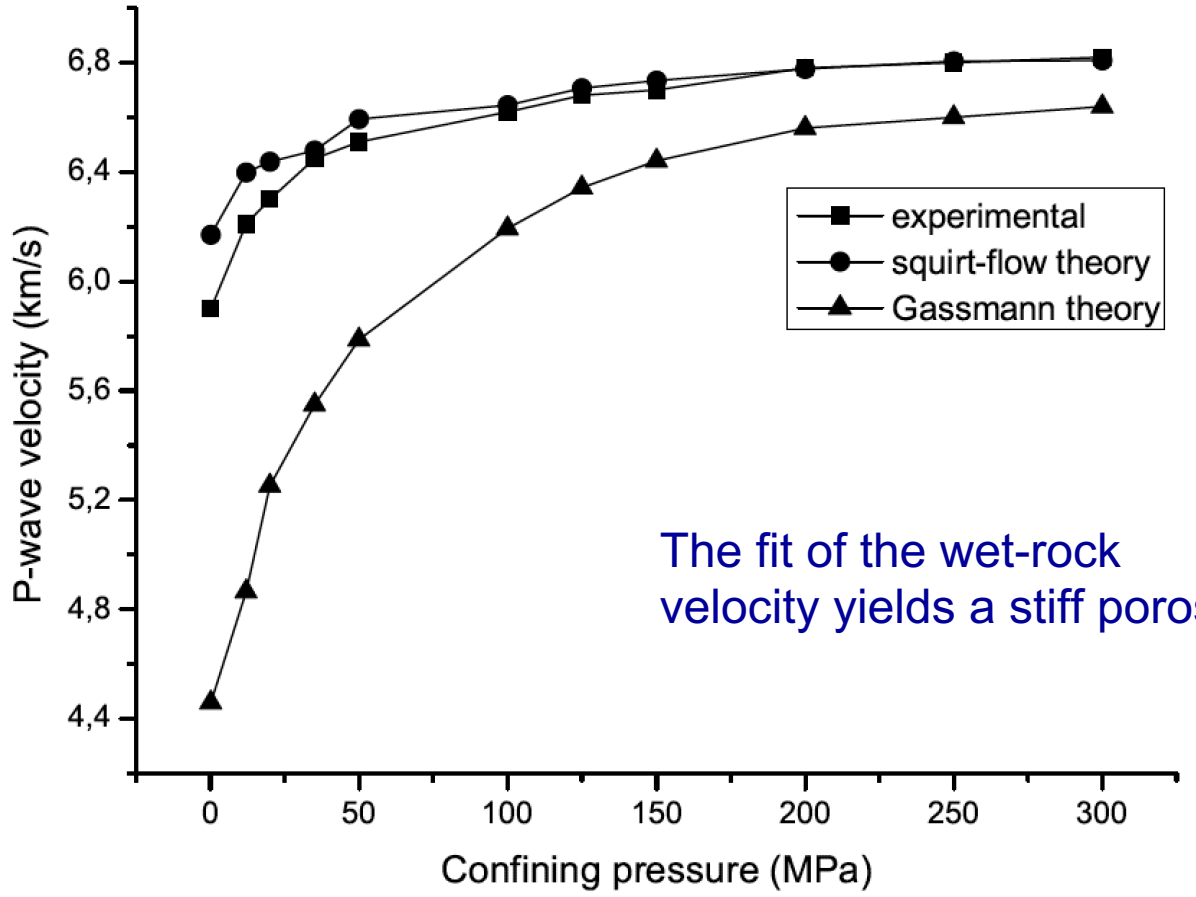

The fit of the wet-rock velocity yields a stiff porosity = 5 %

Carcione, J. M., and Gurevich, B., 2011. *Differential form and numerical implementation of Biot's poroelasticity equations with squirt dissipation*, Geophysics, 76, N55-N64.

Dry-rock moduli

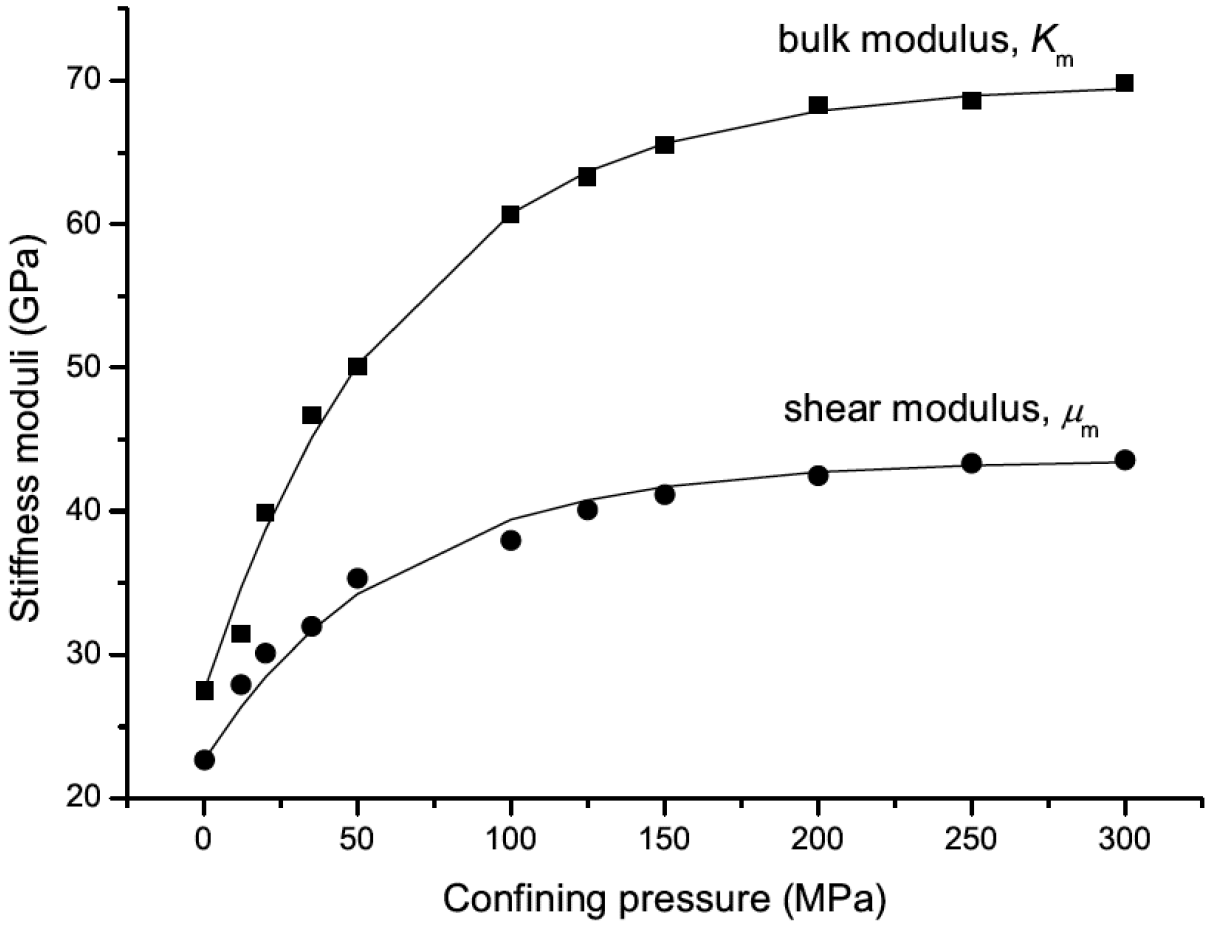

This fit corresponds to $\eta = \infty$, i.e., $\mu_B = \mu_0$

Water properties

From National Institute of Standards and Technology (NIST)

density

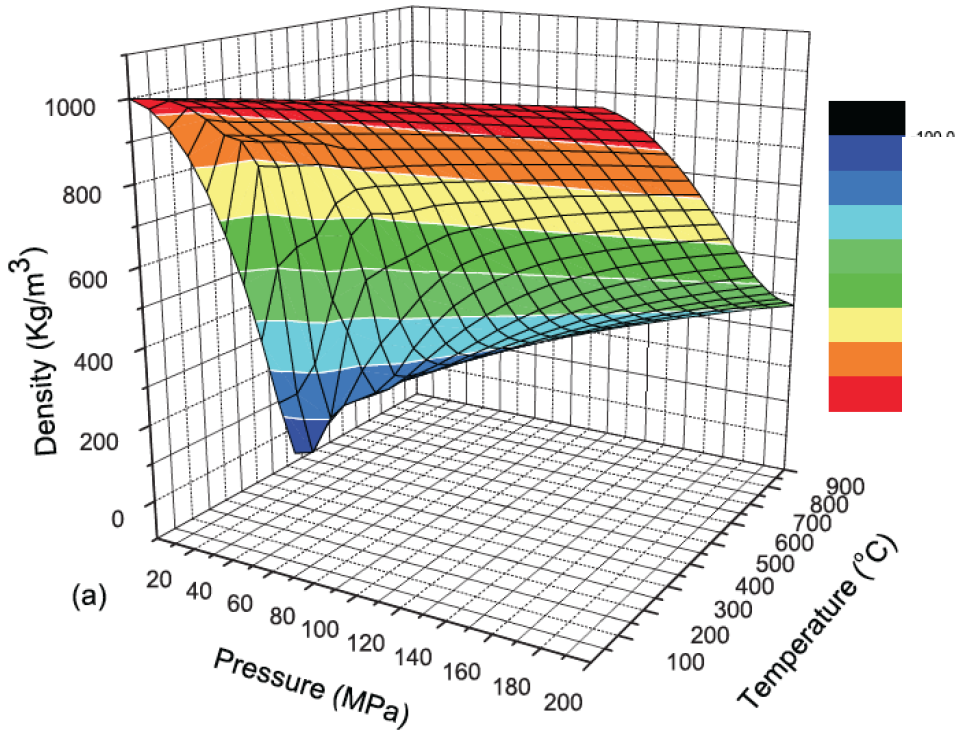

sound velocity

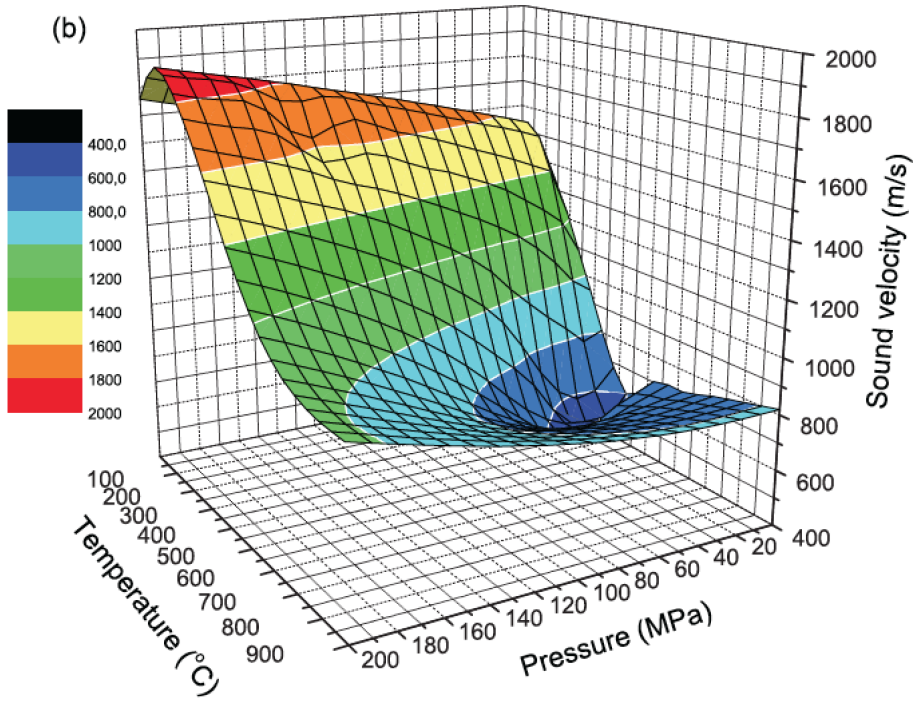

Wave velocities

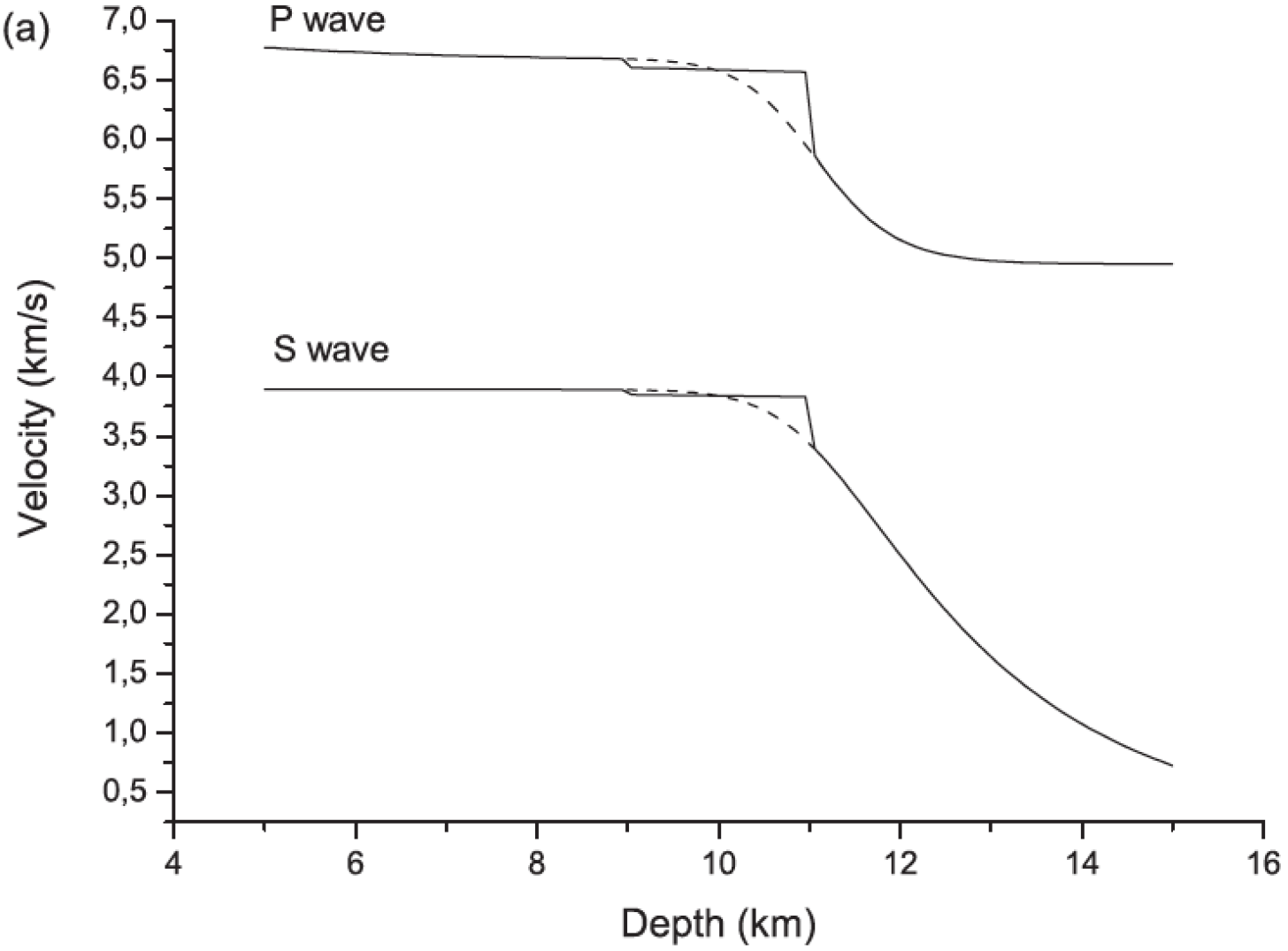

Attenuation

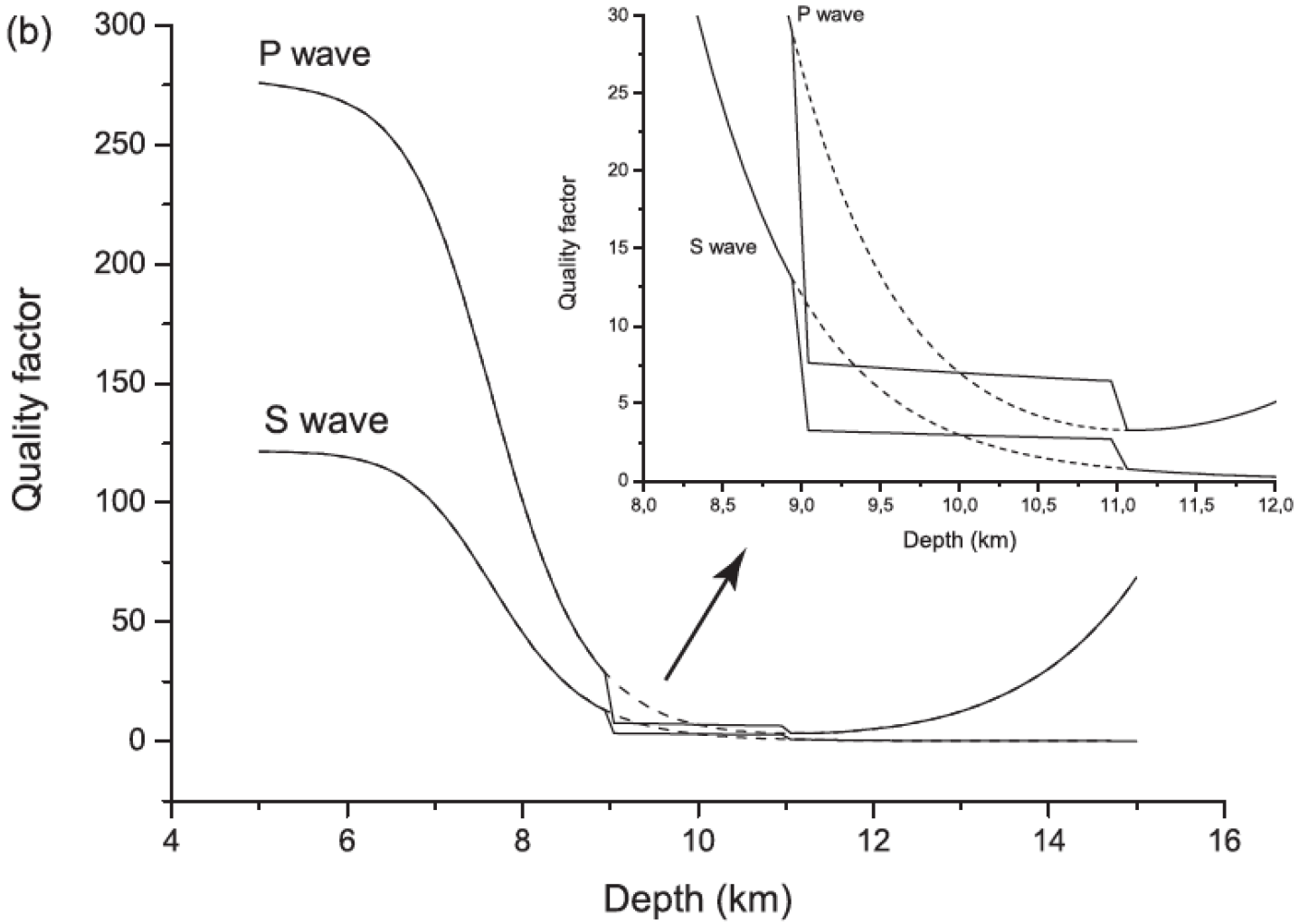

Velocities vs frequency (800 °C)

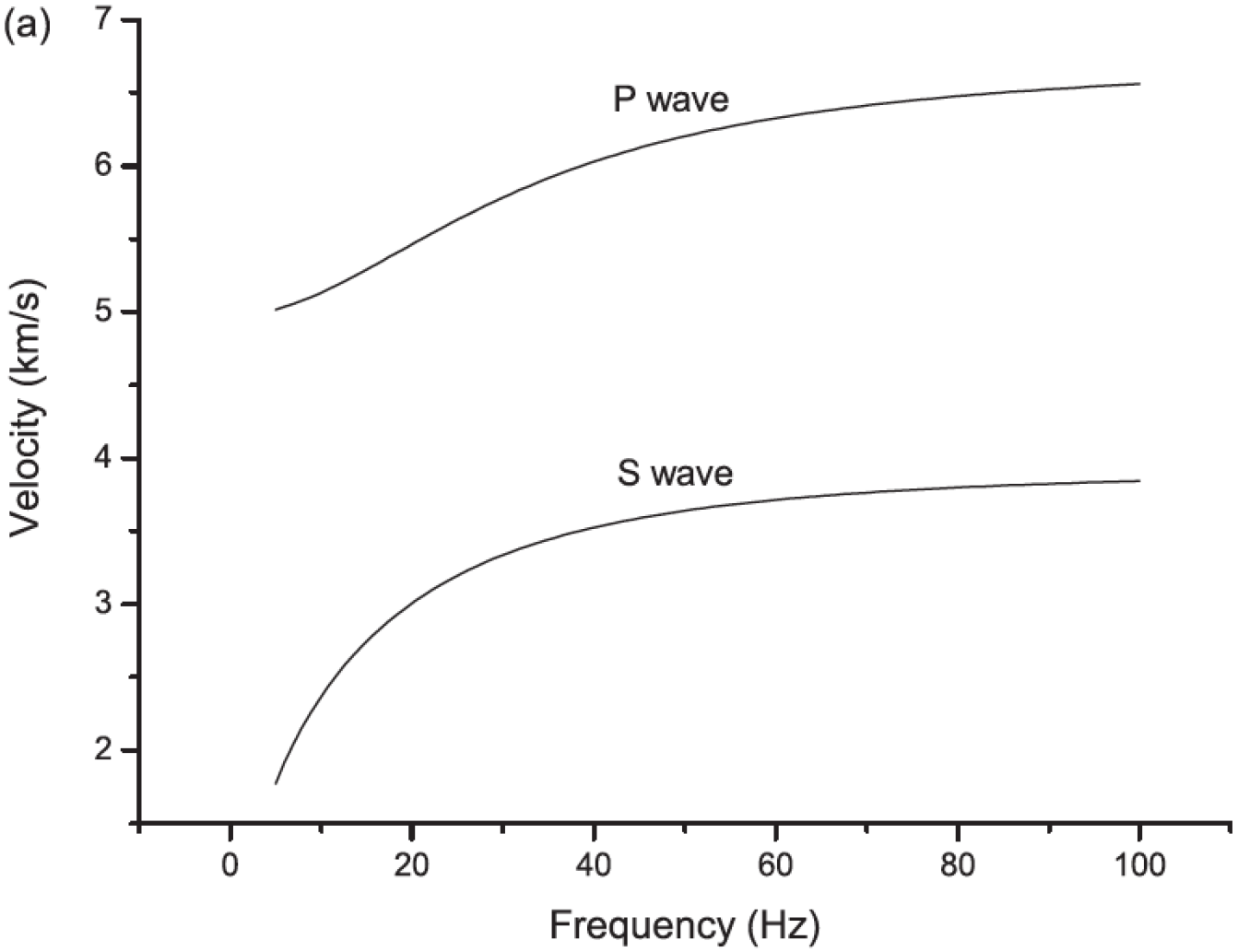

Q vs frequency (800 °C)

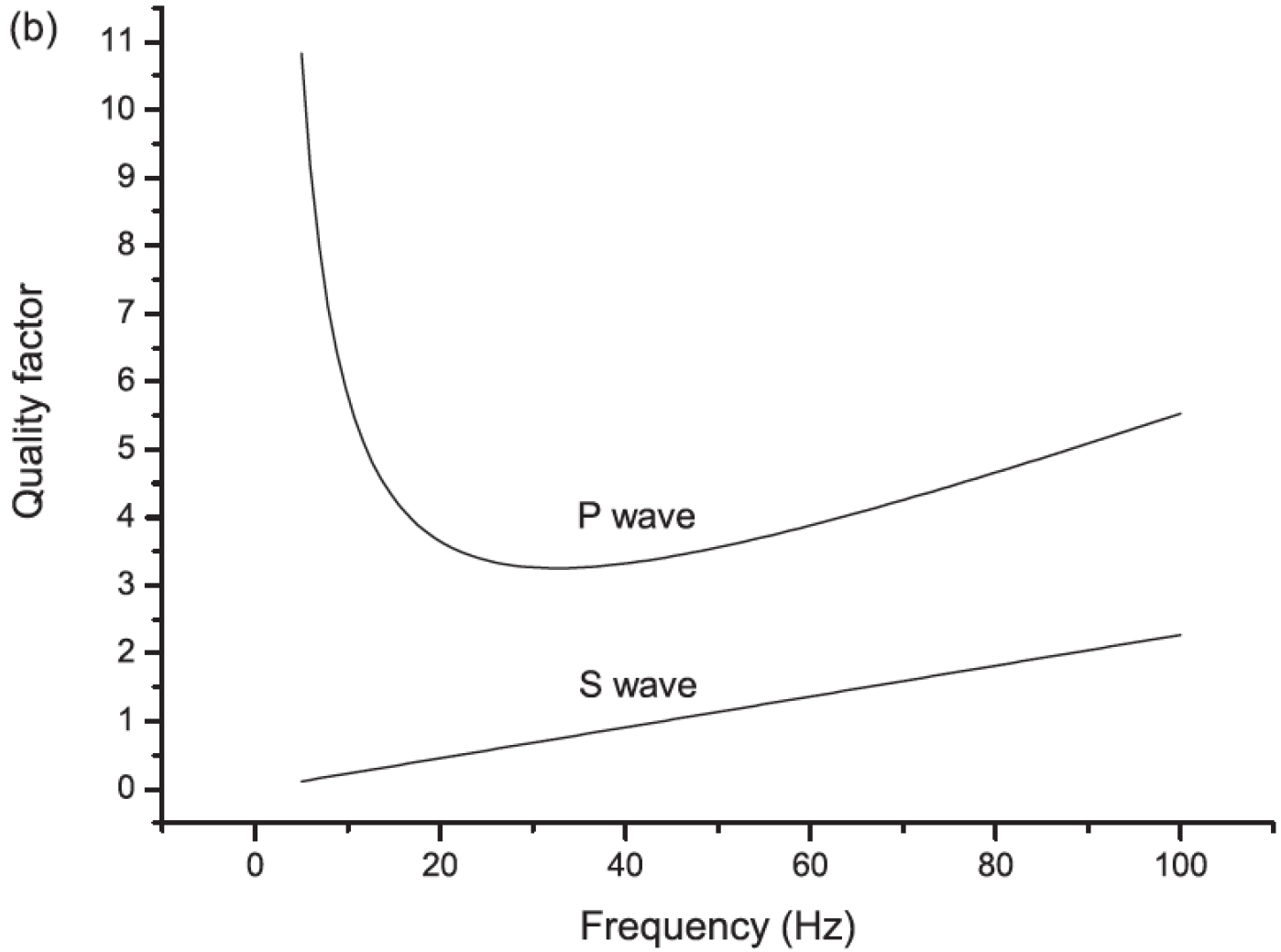

Cross-well simulation

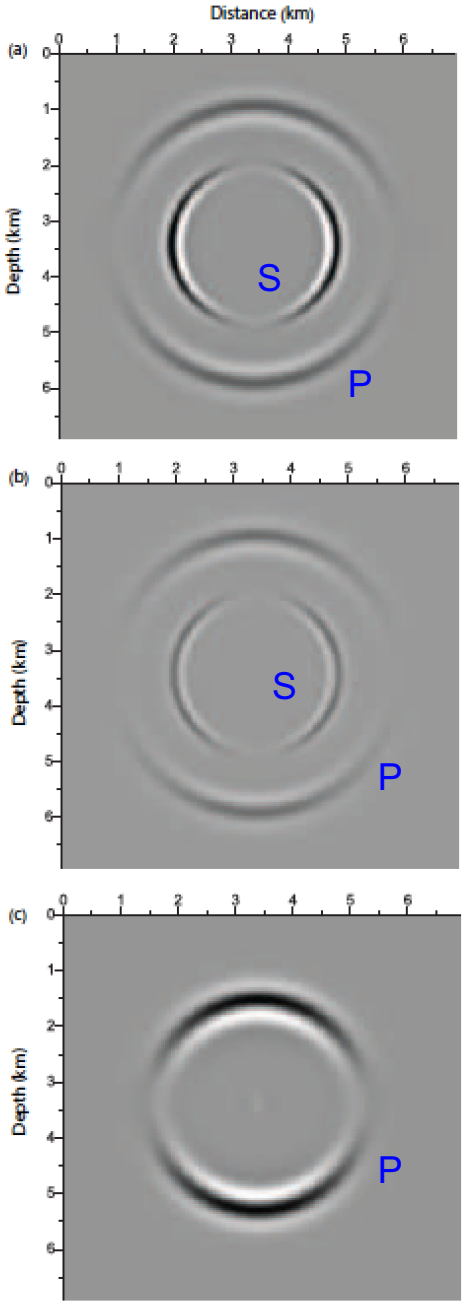

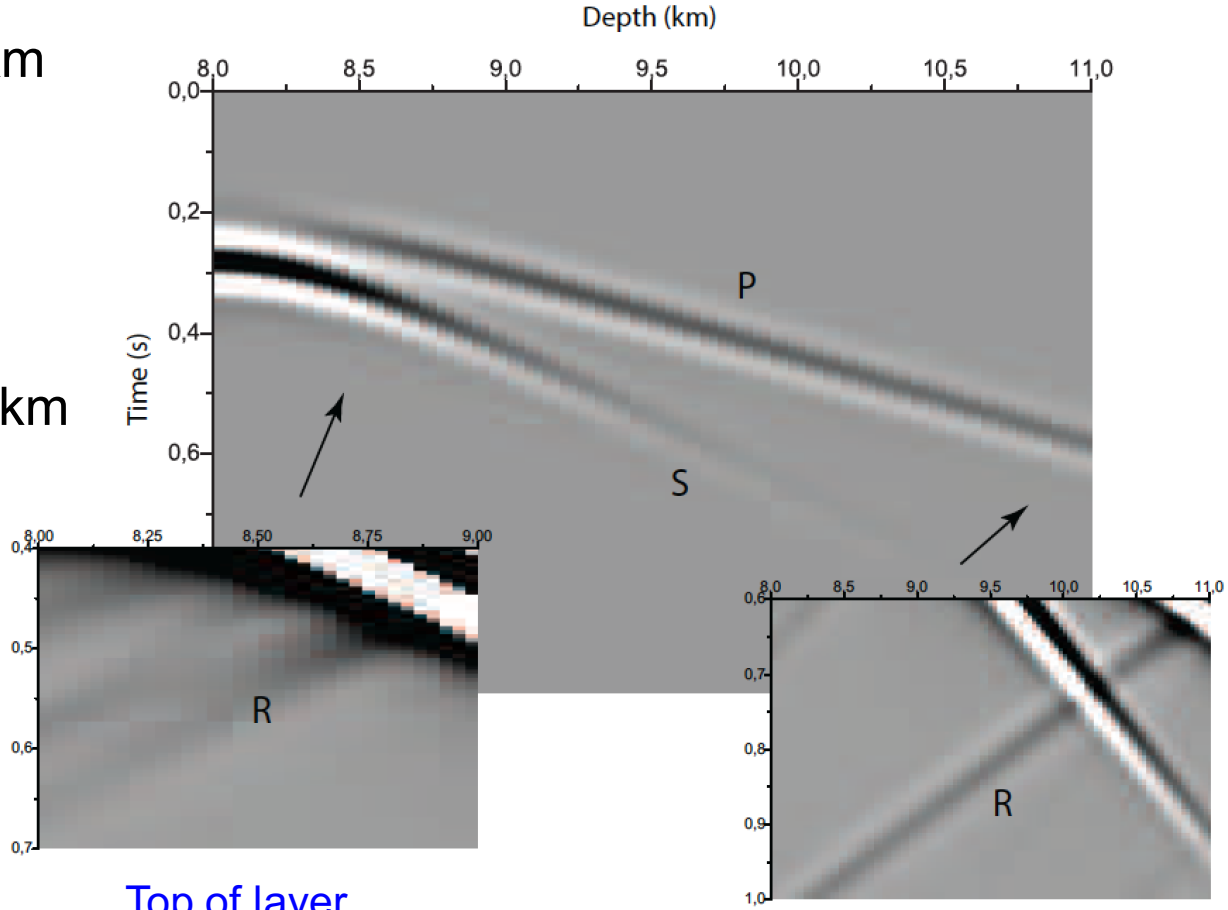

Conclusions

The abrupt brittle-plastic transition is believed to be the lower limit of seismicity and may be an indication of geothermal activity, since its reflectivity may reveal the presence of partial melting and/or overpressured fluids.

Combining a Burgers mechanical kernel and the Arrhenius equation to calculate the flow viscosity, we obtain a realistic rheological model describing the transition. The model can be 3D and include anisotropy, seismic wave attenuation and poroelasticity.

There is high attenuation and velocity dispersion at the critical temperature, where partial melt occurs, and can be used as an indication of the presence of the brittle-ductile transition.

At higher temperatures the medium becomes an anisotropic fluid (no S waves).

The wet-rock seismic velocities can explicitely be computed as a function of pore and confining pressures and the water bulk modulus, with water at normal, critical and supercritical conditions.

Numerical simulations (seismic modeling) can be performed by the introduction of memory variables.

Carcione, J. M., and Poletto, F., 2013, *Seismic rheological model and reflection coefficients of the brittle-ductile transition*, Pure and Applied Geophysics, 170, 2021-2035.

Carcione, J. M., Poletto, F., Farina, B., and Craglietto, A., 2014, *Simulation of seismic waves at the brittle-ductile transition based on the Burgers model*, Solid Earth, **5**, 1001-1010.

Carcione, J. M., Poletto, F., Farina, B., and Craglietto, A., *The Gassmann-Burgers model to simulate seismic waves at the Earth crust and mantle*, submitted to Pageoph.

Carcione, J. M., and Poletto, F., The Burgers/squirt-flow seismic model of the crust and mantle, in preparation

1817 **1921** **1989** **2012**